The *ncl-1* Gene and Genetic Mosaics of *Caenorhabditis elegans*

Edward M. Hedgecock* and Robert K. Herman†

**Department of Biology, Johns Hopkins University, Baltimore, Maryland 21218 and †Department of Genetics and Cell Biology, University of Minnesota, St. Paul, Minnesota 55108*

Manuscript received June 26, 1995
Accepted for publication August 15, 1995

ABSTRACT

A *ncl-1* mutation results in enlarged nucleoli, which can be detected in nearly all cells of living animals by Nomarski microscopy. Spontaneous mitotic loss of a *ncl-1(+)*-containing free duplication in an otherwise homozygous *ncl-1* mutant animal results in mosaicism for *ncl-1* expression, and the patterns of mosaicism lead us to conclude that *ncl-1* acts cell autonomously. The probability of mitotic loss of the duplication *sDp3* is approximately constant over many cell divisions. About 60% of the losses of *sDp3* at the first embryonic cell division involve nondisjunction. Frequencies of mitotic loss of different *ncl-1(+)*-bearing free duplications varied over a 200-fold range. The frequencies of mitotic loss were enhanced by a chromosomal *him-10* mutation. We have used *ncl-1* as a cell autonomous marker in the mosaic analysis of *dpy-1* and *lin-37*. The focus of action of *dpy-1* is in hypodermis. A mutation in *lin-37* combined with a mutation in another gene results in a synthetic multivulva phenotype. We show that *lin-37* acts cell nonautonomously and propose that it plays a role, along with the previously studied gene *lin-15*, in the generation of an intercellular signal by *hyp7* that represses vulval development.

JUST as the function of a gene can be tested by ascertaining the effects of inactivating the gene in a living organism, so can the cell specificity of a gene's function be tested by the analysis of genetic mosaics, in which one can ascertain the effects of inactivating the gene in subsets of cells. Most genetic mosaics of the nematode *Caenorhabditis elegans* have been generated by the spontaneous somatic loss of free chromosome fragments (HERMAN 1984; for review, see HERMAN 1989), called free duplications. In this technique, the normal chromosomes are homozygous for a recessive allele of the gene to be analyzed, and the free duplication carries a dominant (almost always wild-type) allele. *C. elegans* chromosomes are holocentric (ALBERTSON and THOMSON 1982, 1993), which means that the mitotic spindle fibers attach over large extents of the metaphase chromosomes rather than at specific localized sites. Thus the problem of unstable acentric fragments does not arise, and free duplications of many different regions of the genome segregate fairly regularly at mitosis. Free duplications are subject to spontaneous mitotic loss at low frequency, however, and mitotic duplication loss generates a homozygous recessive mutant clone in a background of duplication-bearing cells, a genetic mosaic.

In characterizing a mosaic animal it is usually important to have a cell autonomous genetic marker on the duplication in addition to the gene under study. A good genetic marker enables one to determine with confidence the genotypes of many different cells in the mosaic animal. In addition to being cell autonomous, an ideal cell marker would be scoreable in all cells of living animals of various ages, would have no effect on other possible mutant phenotypes to be analyzed and would exhibit no perdurance, which is the persistence and transmission of the gene product to descendant cells after the gene is no longer present (GARCIA-BELLIDO and MERRIAM 1971). We show in this article that a *ncl-1* gene mutation has essentially all the properties of an ideal cell marker. We have exploited *ncl-1* as a cell marker to help reveal some features about duplication loss as well as measure the frequencies of mitotic loss of several different free duplications. There is considerable interest in taking advantage of the virtues of *ncl-1* as a cell marker in the mosaic analysis of genes that are not closely linked to it and therefore not normally found on the same free duplication. We describe one approach to this problem: the fusing of a *ncl-1(+)*-bearing free duplication to an unlinked free duplication to give a new free duplication carrying both *ncl-1(+)* and the gene of interest.

We illustrate the use of *ncl-1* as a cell marker in the mosaic analysis of two genes. One of these, *lin-37*, is defined by a mutation that affects *C. elegans* vulva development. The hermaphrodite vulva is formed during late larval development. Each of six cells situated in a longitudinal row on the ventral side of the hermaphrodite is capable of generating descendants that contribute to the vulva (for reviews, see HORVITZ and STERNBERG 1991; STERNBERG 1993). These six cells are called the vulval precursor cells (VPCs), although normally only three VPCs contribute to the vulva; the remaining

Corresponding author: Robert K. Herman, Department of Genetics and Cell Biology, University of Minnesota, 250 BioScience Center, 1445 Gortner Ave., St. Paul, MN 55108.
E-mail: bob-h@molbio.cbs.umn.edu

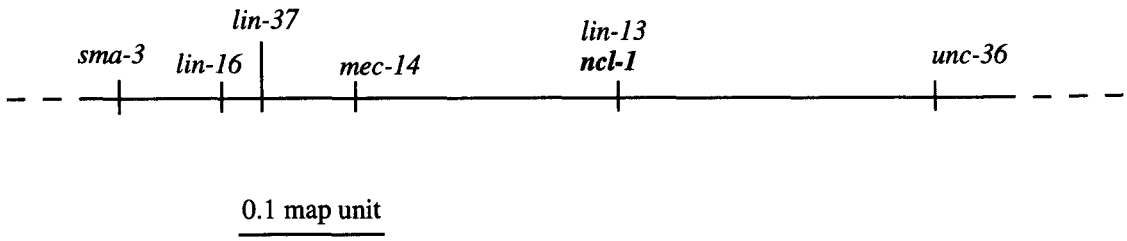

FIGURE 1.—Genetic map in the region of *ncl-1 III*. The map is based in part on data presented in Table 1 and in part on other data available from ACeDB (A *C. elegans* database, compiled by R. DURBIN and J. THIERRY-MIEG, MRC Laboratory of Molecular Biology, Cambridge, England).

three take an alternative developmental path: they fuse, usually after dividing once, with the large multinuclear hypodermis, hyp7, that surrounds them and the developing vulva, and covers most of the worm's body except for the head and tail. The three VPCs selected for vulva development are those closest to the uterine anchor cell. The anchor cell produces an intercellular signal that induces three VPCs to generate 22 descendants, which undergo cell fusions and intricate morphogenetic movements to produce the vulva.

In multivulva (Muv) mutant hermaphrodites, all six VPCs commit to producing descendants that form the vulva rather than fusing with hyp7 (FERGUSON and HORVITZ 1985, 1989; FERGUSON *et al.* 1987); the extra vulval cells that are generated typically form ectopic ventral protrusions called pseudovulvae. In an earlier mosaic analysis, we showed that the Muv gene *lin-15* behaved cell nonautonomously, and we proposed that *lin-15(+)* expression is required in the hyp7 syncytium to repress an intrinsic vulval program in the VPCs (HERMAN and HEDGECOCK 1990). According to this view, the inducing signal from the anchor cell must then countermand the hyp7 inhibitory signal for three of the six VPCs. FERGUSON and HORVITZ (1989) have identified and characterized a set of mutations referred to as silent or synthetic Muv. None of the silent Muv mutations alone results in a Muv phenotype, but hermaphrodites carrying two mutations, one in class A and one in class B, are Muv. FERGUSON and HORVITZ (1989) have proposed that the Muv phenotype caused by synthetic Muv mutations results from defects in two functionally redundant pathways. Indeed, many alleles of *lin-15* are silent Muv mutations, some class A and others class B; the *lin-15* locus was recently cloned and shown to produce two nonoverlapping transcripts corresponding to the two genetically defined functions (CLARK *et al.* 1994; HUANG *et al.* 1994). The *lin-15* mutations that result in a Muv phenotype on their own affect both transcripts. The *lin-37* gene is defined by a silent Muv class B mutation. We show in this article that *lin-37* also behaves cell nonautonomously and propose that it also acts within hyp7 to help generate the intercellular repression of vulval development by the VPCs.

The second gene we analyzed in mosaics is *dpy-1*, mutations in which result in greatly shortened animals of approximately normal girth (BRENNER 1974). The

TABLE 1

Multifactor map data

Genotype of heterozygote	Recombinant phenotype	No.	Genotype of recombinant chromosome
sma-3 ncl-1 unc-36/+ + +	Sma non-Unc	1/1	*sma-3 + +*
	Unc non-Sma	4/7	*+ ncl-1 unc-36*
		3/7	*+ + unc-36*
sma-3 + ncl-1 unc-36/+ lin-16 + +	Sma non-Unc	1/5	*sma-3 lin-16 + +*
		2/5	*sma-3 + + +*
		2/5	*sma-3 + ncl-1 +*
	Unc non-Sma	4/4	*+ lin-16 ncl-1 unc-36*
sma-3 + ncl-1 unc-36/+ lin-37 + +[a]	Sma non-Unc	1/2	*sma-3 + + +*
		1/2	*sma-3 + ncl-1 +*
	Unc non-Sma	2/3	*+ lin-37 + unc-36*
		1/3	*+ lin-37 ncl-1 unc-36*
sma-3 + ncl-1 unc-36/+ lin-13 + +	Unc non-Sma	19/32	*+ + ncl-1 unc-36*
		13/32	*+ lin-13 + unc-36*
sma-3 + ncl-1 unc-36/+ mec-14 + +	Sma non-Unc	6/15	*sma-3 mec-14 + +*
		3/15	*sma-3 + + +*
		6/15	*sma-3 + ncl-1 +*

[a] This strain was also homozygous for *lin-8 II*; the double mutant *lin-8; lin-37* has a multivulva phenotype, whereas *lin-37* by itself confers a wild-type phenotype.

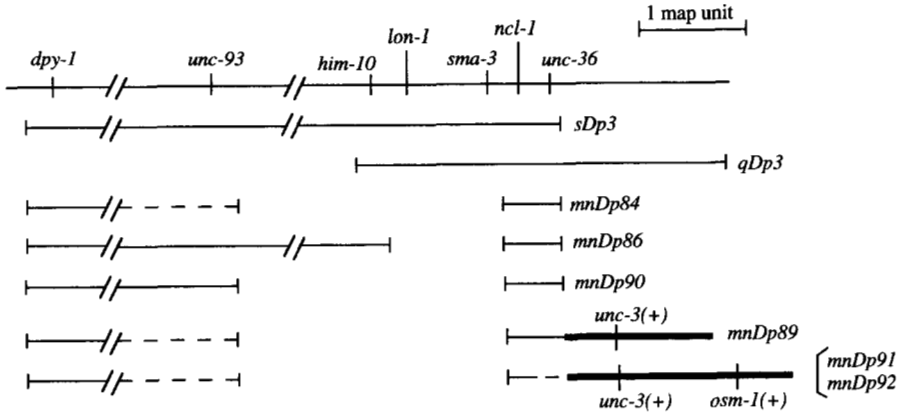

FIGURE 2.—Extents of various duplications used in this work. Duplications *mnDp84* and *mnDp86* were derivatives of *sDp3*, and *mnDp90* was derived from *mnDp86*. We showed that *qDp3* carries *him-10(+)*, but *mnDp84* has not been tested with respect to the *unc-93* locus. Duplication *mnDp89* was generated by the fusion of *mnDp84* and *mnDp14*, and *mnDp91* and *mnDp92* were generated by the fusion of *mnDp90* and *mnDp14*. All three fused duplications carry *unc-3(+) X*. Duplication *mnDp89* does not carry *osm-1(+) X*, but *mnDp91* and *mnDp92* do. The latter two duplications have not been checked with respect to either *unc-93* or *unc-36*. The representations of the three fused duplications are highly schematic; the junctions and orientations of the different components of each fused duplication are unknown.

focus of action of this gene also appears to be in hypodermis; mosaic analysis has uncovered specific effects traceable to head and tail hypodermal cells in addition to the large hyp7 syncytium.

MATERIALS AND METHODS

General genetic methods, genes, alleles and rearrangements: Growth media, EMS mutagenesis and culture and mating techniques were as described by BRENNER (1974) and SULSTON and HODGKIN (1988). Nematode strains were grown and mated at 20°. We have followed standard *C. elegans* genetic nomenclature (HORVITZ *et al.* 1979). Genes, mutations and chromosome rearrangements used (references for most are given by HODGKIN *et al.* 1988) were the following: LG (linkage group) II: *lin-8(n111)*. LG III: *dpy-1(e1), unc-93(e1500), unc-93(e1500n224)*, which we refer to as *unc-93(0), him-10(e1511ts), lon-1(e185), sma-3(e491), lin-16(e1743), lin-37(n758), mec-14(u55), ncl-1(e1865), lin-13(n387), unc-36(e251), dpy-19(e1259), glp-1(q339), sDp3(III;f)* (ROSENBLUTH *et al.* 1985), *qDp3(III;f)* (AUSTIN and KIMBLE 1987), *nDf16* (THOMAS *et al.* 1990), *qC1* (AUSTIN and KIMBLE 1989). LG IV: *him-8(e1489)*. LG V: *him-5(e1467)*. LG X: *him-4(e1267), unc-3(e151), osm-1(p808), sup-10(n983), mnDp30(X;f)* (HERMAN *et al.* 1979), *mnDp14(X;f)* (HERMAN 1984). The derivations of additional free duplications are described below. The *osm-1* marker was scored with respect to its effect on dye filling of amphid and phasmid neurons (PERKINS *et al.* 1986).

Genetic mapping of *ncl-1*: We have mapped *ncl-1* to a site near the middle of LG III, between *sma-3* and *unc-36* (Figure 1). The results of three- and four-factor crosses involving closely linked markers in this interval are given in Table 1. The phenotype scored for *lin-13* and *lin-37* (the latter in combination with *lin-8*) was multivulva or Muv (FERGUSON and HORVITZ 1985, 1989); *lin-16* results in a thin, sterile uncoordinated animal; and *mec-14* abolishes the response to light touch of an eyebrow hair (CHALFIE and SULSTON 1981). We showed that *ncl-1/Df* hermaphrodites are Ncl, viable and fertile: *ncl-1 unc-36; mnDp90; him-8* males were mated with *nDf16/qC1 dpy-*

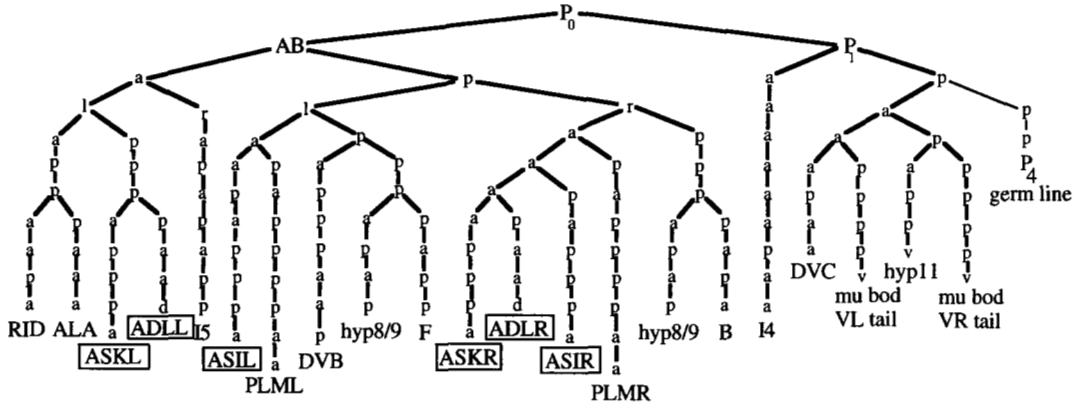

FIGURE 3.—The lineages of 21 somatic cells that were used to monitor frequency of duplication loss. The origin of P_4, which gives rise to the germline, is also shown. Each cell is drawn below its mother cell, and its lineage can be read directly from the diagram, where a, p, l, r, d and v refer to anterior, posterior, left, right, dorsal and ventral daughters, respectively. Thus, for example, the last common ancestor of RID, ALA, ASKL and ADLL is the left daughter of the anterior daughter of AB, which is designated ABal, and the lineal name of RID is ABalappaapa. In one set of experiments, animals were scored for mosaicism of the six amphidial neurons that are boxed in the diagram, *viz.*, ASKL, ADLL, ASIL, ASKR, ADLR and ASIR. The 21 somatic cells shown are generated by a total of 140 cell divisions. The lineages of hyp8 and hyp9 are ambiguous; either of the two indicated cells can become the more anterior cell, which is designated hyp8.

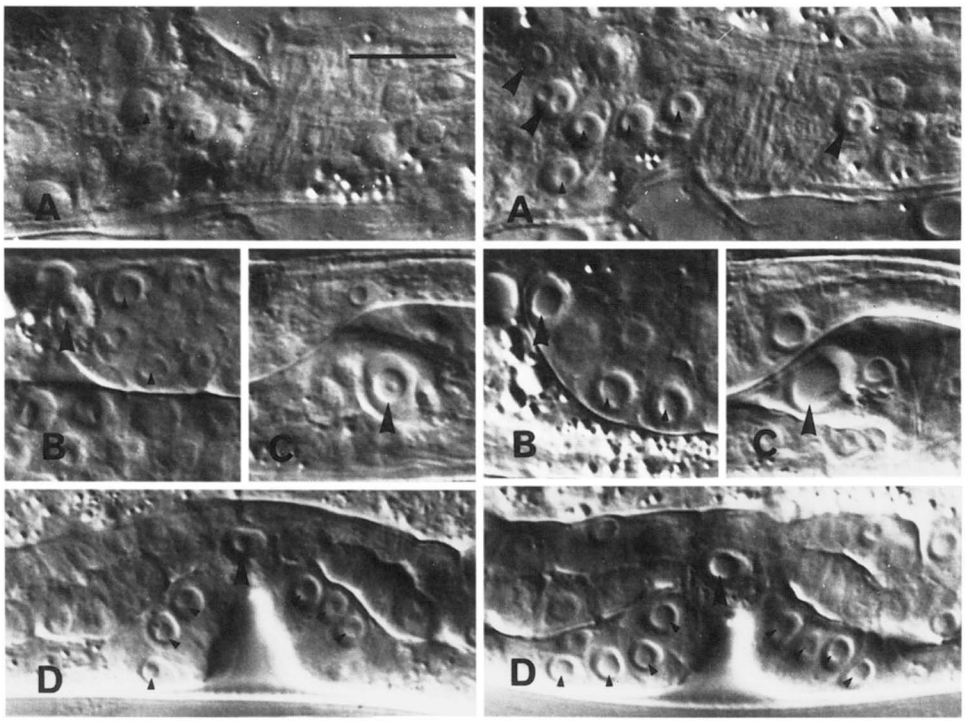

FIGURE 4.—Nomarski photomicrographs comparing nucleoli in wild-type (left panels) and *ncl-1* homozygotes (right panels). (A) Nerve ring ganglia showing nucleoli of sensory and other neurons. In wild-type, a small, fused nucleolus (small arrowheads) is visible in each neuronal nucleus. In *ncl-1,* these neurons have either a large, fused nucleolus (small arrowhead) or, less frequently, two distinct nucleoli (large arrowhead). (B) Distal gonad showing nucleoli of distal tip cell (large arrowhead) and germline cells (small arrowheads). (C) Excretory cell nucleoli (large arrowheads). (D) Developing vulva and uterus showing nucleoli of vulval cells (small arrowheads) and uterine anchor cell (large arrowheads). Right lateral aspect of new L4 hermaphrodites. Scale bar, 10 μm.

19 glp-1 hermaphrodites, and Unc-36 hermaphrodite progeny, genotype *nDf16/ncl-1 unc-36,* were picked and scored.

Strain constructions: Most strains were constructed by standard methods (BRENNER 1974). A male stock of genotype *dpy-1 ncl-1; sDp3* was maintained and used in some strain constructions. One of the Unc non-Sma recombinants arising from a *lin-8 II; sma-3 ncl-1 unc-36/lin-37* hermaphrodite parent (Table 1) was used to initiate a *lin-8 II; lin-37 ncl-1 unc-36 III* strain. A *lin-8; dpy-1 lin-37 ncl-1 unc-36* strain was derived as follows: *lin-8; lin-37 ncl-1 unc-36* hermaphrodites were mated with *dpy-1 ncl-1; sDp3* males; wild-type hermaphrodites were picked, and several of their Muv (requiring both *lin-8* and *lin-37* to be homozygous [FERGUSON and HORVITZ 1989]) Unc-36 segregants were picked; animals of the desired genotype were found among their progeny. The duplication *sDp3* was added to *lin-8; lin-37 ncl-1 unc-36 and lin-8; dpy-1 lin-37 ncl-1 unc-36* genetic backgrounds by mating hermaphrodites of each of these genotypes with *dpy-1 ncl-1; sDp3* males and selecting wild-type hermaphrodite progeny. Hermaphrodites bearing *sDp3* were recognized on the basis of the ratios of phenotypes of their self-progeny, among which were found animals of the desired genotypes.

The construction of a *lin-8 II; dpy-1 unc-93(0) lin-37 ncl-1 unc-36 III; sDp3; sup-10(n983) X* strain will be described. The *sup-10(n983)* mutation, which is essentially recessive to *sup-10(+),* confers a phenotype referred to as rubberband (GREENWALD and HORVITZ 1986): animals tend to be long, thin and uncoordinated and recoil and then quickly relax when touched. The rubberband phenotype is suppressed recessively by *unc-93(0).* Males of genotype *unc-93(0); him-5; sup-10/0* were mated with *dpy-1 unc-93(0); sup-10* hermaphrodites. Wild-type male progeny, genotype *dpy-1 unc-93(0)/unc-93(0); him-5/+; sup-10/0,* were mated with *lin-8; dpy-1 lin-37 ncl-1 unc-36* hermaphrodites. Dpy non-Unc-36 non-Muv hermaphrodite progeny were picked, from which many Dpy non-Unc-36 rubberband hermaphrodites were picked individually to separate plates. From broods that contained Dpy Unc-36 animals, many Dpy non-Unc-36 non-rubberband (suppressed) hermaphrodites were picked individually. Among the broods of such animals, a Dpy Unc-36 Muv non-rubberband segregant was found and picked to establish a *lin-8; dpy-1 unc-93(0) lin-37 ncl-1 unc-36; sup-10* strain. The presence of *ncl-1* was confirmed by Nomarski microscopy. The presence of *sup-10* was confirmed by mating to N2 males, which yielded rubberband male progeny. The presence of *unc-93(0)* was confirmed (since the rubberband phenotype is more difficult to score in Dpy Unc-36 animals) by mating to *unc-93(0); him-5; sup-10/0* males and finding only non-rubberband progeny. Next, *unc-93(0); him-5; sup-10/0* males were mated with *lin-8; dpy-1 unc-93(0) lin-37 ncl-1 unc-36; sup-10* hermaphrodites. Wild-type male progeny were then mated with *lin-8; dpy-1 lin-37 ncl-1 unc-36; sDp3* hermaphrodites. From an efficient mating (yielding a high proportion of male progeny), many wild-type hermaphrodite progeny were picked individually. Animals of genotype *lin-8; dpy-1 lin-37 ncl-1 unc-36/dpy-1 unc-93(0) lin-37 ncl-1 unc-36; sDp3; sup-10/+* were identified from the phenotypes of their broods; rubberband segregants were picked, among which animals of genotype *lin-8; dpy-1 unc-93(0) lin-37 ncl-1 unc-36; sDp3*[*dpy-1(+) unc-93(+) lin-37(+) ncl-1(+) unc-36(+)*]*; sup-10* were identified. These animals are non-Dpy rubberband non-Muv non-Ncl non-Unc-36; their nullo-*sDp3* self-progeny are Dpy non-rubberband Muv Ncl Unc-36.

Pruning free duplications: Young adult *sma-3 ncl-1 unc-36; sDp3* hermaphrodites were exposed to 3800 roentgens (r) of gamma rays from a ^{137}Cs source, and exceptional Sma non-Unc progeny were picked to identify duplications that retained *unc-36(+)* but lacked *sma-3(+).* Two such duplications, which were recovered at a frequency of about one per 2000 duplication-bearing progeny screened, were *mnDp84* and *mnDp86,* both of which carry *ncl-1(+).* The genetic background of each of these duplications was changed by mating the *sma-3 ncl-1 unc-36; Dp* hermaphrodites with *ncl-1 unc-36/+ +* males; *sma-3 ncl-1 unc-36/ncl-1 unc-36; Dp* hermaphrodite progeny were identified, from which *ncl-1 unc-36; Dp* segregants were recovered. For each duplication, a *dpy-1 ncl-1 unc-36; Dp* strain and a *lon-1 ncl-1 unc-36; Dp* strain were established, and for each duplication, the former were non-Dpy non-Unc and the latter were Lon non-Unc; thus both *mnDp84* and *mnDp86* carry *dpy-1(+)* and not *lon-1(+).* Similarly, *him-10*

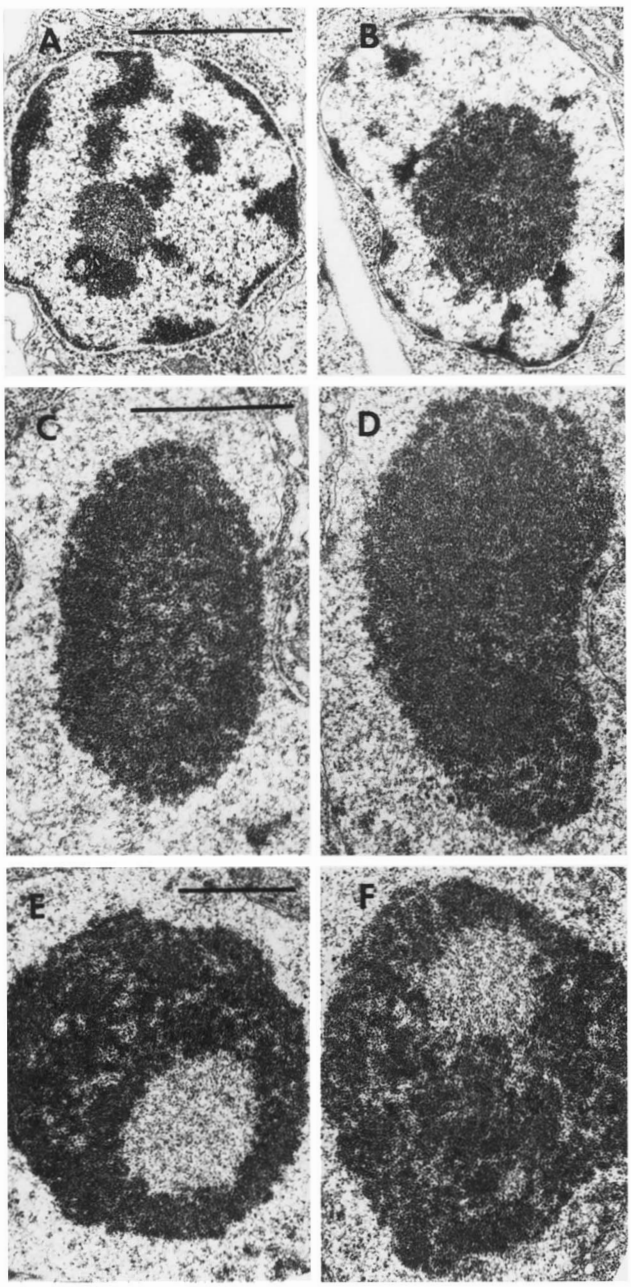

FIGURE 5.—Electron micrographs comparing nucleoli in wild-type (A, C, E) and *ncl-1* adults (B, D, and F). (A and B) Motorneuron nuclei showing a lightly stained nucleolus and darker heterochromatin. (C and D) Body muscle nuclei. (E and F) Germline nuclei. Scale bars, 1 μm.

ncl-1 unc-36; Dp strains were established to show that *mnDp86* carries *him-10(+)* and that *mnDp84* does not (Figure 2). Individual *him-10 ncl-1 unc-36; mnDp86* hermaphrodites were picked to separate plates; among 200 animals, one was found that was Him non-Unc, and it transmitted an altered free duplication, called *mnDp90*, which lacks *him-10(+)* but retains *ncl-1(+)* and *unc-36(+)*. The *him-10(+)* gene was probably lost as a consequence of deletion formation, which is why we have given the duplication a new name; many free duplications have been shown to be subject to deletion-formation at high frequency (HERMAN 1984; MCKIM and ROSE 1990; VILLENEUVE and MEYER 1990). However, we cannot rule out the possibility that *mnDp90* picked up the *him-10 III* mutation by homologous recombination with a *him-10* chromosome. The *mnDp90*-bearing males are fertile (unlike *mnDp84*-bearing males, a *him-5* stock of which was tested repeatedly for male mating), and the duplication has been put in several genetic backgrounds (some including *him-8*, for generating males at high frequency). We showed that *mnDp90* carries *dpy-1(+)* and *unc-93(+)* but not *lin-37(+)*. The following crosses were used to show that *mnDp90* carries *unc-93(+)*. Males of genotype *dpy-1 ncl-1; mnDp90; him-8* were mated with *dpy-1 unc-93(e1500)* hermaphrodites. Wild-type hermaphrodite progeny were picked, among whose self-progeny were found *dpy-1 unc-93; mnDp90* hermaphrodites; these animals were largely wild-type with respect to locomotion (*unc-93(e1500)* is weakly semi-dominant) and non-Egl and segregated appropriate self-progeny.

Fusing unlinked free duplications: The following procedure was used to generate fusions of *mnDp90(III;f)* and *mnDp14(X;f)*. First, a strain carrying both duplications was constructed: *dpy-1 ncl-1/+ +; unc-3 osm-1/0; mnDp14*[*unc-3(+) osm-1(+)*] males were mated with *dpy-1 ncl-1; mnDp90; unc-3 osm-1* hermaphrodites. Among the wild-type hermaphrodite progeny, animals of genotype *dpy-1 ncl-1; mnDp90; unc-3 osm-1; mnDp14* were identified on the basis of their progeny ratios and maintained as a stock. The two duplications segregate independently, yielding wild-type, Dpy, Unc and Dpy Unc self-progeny. After exposure to 3300 r of gamma rays, young adult wild-type animals were picked individually to fresh plates, as were several of their wild-type self-progeny. The broods of the latter were screened for the presence of wild-type and Dpy Unc but no Dpy or Unc animals. Approximately 1–2% of the animals tested appeared to carry a fused duplication. For each of eight lines (each descended from a different irradiated hermaphrodite) carrying putative fused duplications, wild-type animals were mated with N2 (wild-type) males, which, as expected, yielded both wild-type (duplication-bearing) and Unc-3 males. The wild-type males were then crossed to *dpy-1 him-10 ncl-1; unc-3 osm-1* hermaphrodites, and wild-type hermaphrodite progeny were picked. Finally, strains homozygous for *him-10* or *him-10(+)* were established for each duplication. Two of the fused duplications generated in this way were *mnDp91* and *mnDp92*, each of which carries *dpy-1(+)*, *ncl-1(+)*, *unc-3(+)* and *osm-1(+)* (Figure 2). The duplication *mnDp89* was generated in a similar way from *mnDp84* and *mnDp14*. It differs from *mnDp91* and *mnDp92* in not carrying *osm-1(+)* and in not being transmissable by males.

DAPI staining: Each animal was deposited individually in a drop of water on a slide, fixed with a drop of Carnoy's (SULSTON and HODGKIN 1988), stained with diamidinophenylindole (ELLIS and HORVITZ 1986) and observed by epifluorescence microscopy.

Nomarski microscopy: Animals were mounted on a slide in a small drop of water on a 5% agar pad by the method described by SULSTON and HODGKIN (1988). Sometimes both water drop and agar contained 10 mM sodium azide as an anesthetic. The Ncl phenotypes of cells were scored by Nomarski differential interference contrast microscopy using either a Zeiss Universal or Zeiss Axioplan microscope. Nuclei were identified using published diagrams (ALBERTSON and THOMSON 1976; SULSTON and HORVITZ 1977; KIMBLE and HIRSH 1979; SULSTON *et al.* 1983, 1988; WHITE *et al.* 1986).

Measuring positions and frequencies of duplication loss: In our first set of experiments, non-Dpy *dpy-1 ncl-1; sDp3* L2-L4 hermaphrodites were picked, and six amphid neurons—ASKL, ADLL, ASIL, ASKR, ADLR and ASIR—of each animal were inspected by Nomarski microscopy for Ncl mosaicism. When a mosaic was found, many lineally related cells (SULSTON and HORVITZ 1977; KIMBLE and HIRSH 1979; SULSTON *et al.* 1983, 1988) were scored to pinpoint as closely as possible the position of duplication loss in the cell lineage, on the

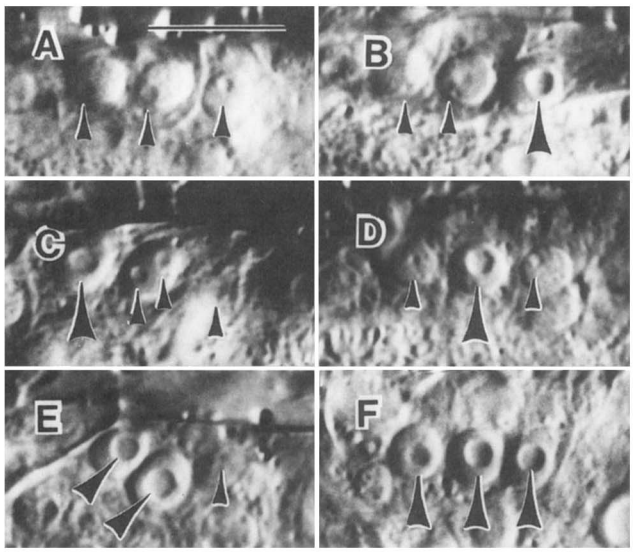

FIGURE 6.—Nomarski photomicrographs comparing nucleoli of neurons ASKL, ADLL and ASIL (left to right in all panels) in non-mosaic and mosaic self-progeny of *dpy-1 ncl-1; sDp3* hermaphrodites. Ncl and non-Ncl cells are shown by large and small arrowheads, respectively. Somatic genotypes are as follows: (A) no duplication loss. (B) ABpl(−), which stands for duplication loss at ABpl. (C) ABalpppap(−). (D) ABalpppp(−). (E) ABa(−). (F) P_0(−). Left lateral aspect of adult hermaphrodites. Scale bar, 10 μm.

assumption that *ncl-1* behaves cell autonomously (see RESULTS). The following additional cells (names and lineages are given by SULSTON and WHITE [1988] and SULSTON *et al.* [1988]) were scored in one or more animals: ADFL, ADFR, AFDL, AFDR, AIBL, AIBR, AINR, ALA, ALML, ALMR, AMshL, AMshR, ASEL, ASER, ASGL, ASGR, ASHL, ASHR, ASJL, ASJR, AUAL, AUAR, AVAL, AVAR, AVDL, AVDR, AVEL, AVER, AVHR, AVJL, AVJR, AVM, AWAL, AWAR, AWBL, AWBR, AWCL, AWCR, B, BAGL, BAGR, CANL, CANR, CEPDL, DVA, DVB, DVC, F, H0L, H0R, HSNL, HSNR, I4, I5, Ka, K', M2L, M2R, M4, OLLL, OLLR, OLLshL, PHAL, PHAR, PHBL, PHBR, PLML, PLMR, PVQL, PVQR, PVR, RID, RIML, RIPL, RIPR, RMDDL, RMDL, RMDR, RMDVL, RMEL, SDQR, SIBVR, SMBDL, SMBVL, U, URBL, URBR, URXL, URXR, exc cell, hyp8, hyp9, hyp10, hyp11, mu anal, rect D, rect VL, rect VR, various mu bod cells and descendants of P5p, P6p, P7p, TL, TR, V4L, V4R, V5L, V5R, V6L, and V6R.

To measure the frequency of duplication loss per cell division in the above experiments, we first note that the frequency of loss was approximately constant throughout the lineage that produces the six selected amphid neurons (see RESULTS). The six neurons are generated by a total of 44 cell divisions from the zygote P_0 (Figure 3), and duplication loss at any of these divisions generates a non-Dpy *ncl-1* mosaic (see RESULTS). The duplication in a nonmosaic animal has thus successfully negotiated 44 cell divisions. In mosaics, however, cell divisions in the lineage following the point of duplication loss were discounted because obviously no loss can occur during these divisions. When the point of loss was not determined exactly, an average position was assumed.

A second procedure was used to measure the frequencies of mitotic loss of several duplications. L2-L4 hermaphrodites were mounted for Nomarski microscopy, and 21 cells, whose lineages are shown in Figure 3, were scored with respect to their Ncl phenotype. Generally no attempt was made to score additional cells or to pinpoint the position of duplication loss within the lineage. The 21 cells are generated by 140 cell divisions (Figure 3). When either *unc-36* (KENYON 1986) or *unc-3* (HERMAN 1984) were in the genetic background, losses at AB or ABp were not possible, however, because they would generate Unc animals, which were not scored, giving a total of 138 cell divisions sampled for a nonmosaic animal. When a particular cell was not scoreable, all cell divisions on its unique branch of the lineage were discounted. When a cell was Ncl, an average position of duplication loss was assumed, and the appropriate number of subsequent cell divisions was subtracted from the total. When two or more related cells were Ncl, a single loss at a common ancestral division was assumed. In this way the total number of losses per total number of cell divisions sampled was measured, on the assumption that the frequency of duplication loss was constant throughout the cell lineage.

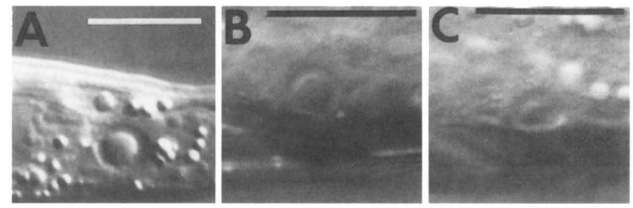

FIGURE 7.—Nomarski photomicrographs of *ncl-1* mosaic animals derived from *dpy-1 ncl-1; sDp3* zygotes. (A) The large Ncl cell is hyp9, and the non-Ncl cell above it is hyp11. (B) A Ncl body muscle cell. (C) A non-Ncl body muscle cell in the same animal shown in B. The two muscle cells in B and C are at bilaterally symmetric positions, left and right of the ventral midline, just posterior to the rectum. Scale bars, 10 μm.

For measuring the frequency of germline transmission of duplications, hermaphrodite parents were transferred daily, and full broods were counted.

RESULTS

The *ncl-1* mutant phenotype: Each of two *ncl-1* mutant alleles was identified among the F_2 offspring of EMS-treated hermaphrodites. The *ncl-1(e1942)* mutation was identified by C. KENYON (personal communication) and confers a phenotype very similar to that of *ncl-1(e1865),* the allele used in this work. Each mutation results in enlarged nucleoli, as observed in most cells at all stages of development by Nomarski differential interference contrast microscopy (Figure 4) or by electron microscopy (Figure 5). Neuronal nucleoli are small in wild-type animals and greatly enlarged in *ncl-1* animals; body muscle and hypodermal nucleoli are also enlarged in *ncl-1* mutants. Intestinal and germline nucleoli are exceptional: they are large in wild-type animals and not markedly larger in *ncl-1* animals. The *ncl-1* mutants exhibit no apparent defects in viability, fertility, development, body morphology or movement. We have mapped *ncl-1* to a site on linkage group III (Table 1; Figure 1). Both mutant alleles are recessive to *ncl-1(+),* and the phenotype of *ncl-1/Df* animals (see MATERIALS AND METHODS) appears to be the same as that of *ncl-1* homozygotes; we suggest that the *ncl-1* mutations are either partial or complete loss-of-function.

Young embryos produced by either wild-type or *ncl-1/+* hermaphrodites do not have discernable nucleoli

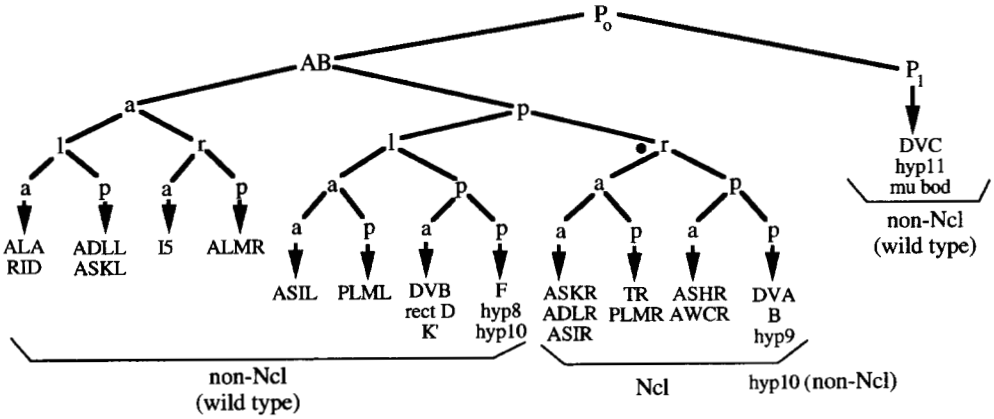

FIGURE 8.—Example of a simple mosaic. It is concluded that the cell ABpr, which is marked by a dot in the lineage tree, failed to transmit the duplication, since all of its indicated descendants were Ncl. The binucleate cell hyp10 is formed by the fusion of two cells, one descended from ABprpp and the other from ABplpp; both hyp10 nuclei were non-Ncl in this animal. Both hyp10 nuclei were Ncl when duplication loss occurred at either AB or AB.p.

in the Nomarski microscope; this includes homozygous *ncl-1* embryos. On the other hand, young embryos even at the two- and four-cell stages produced by homozygous *ncl-1* hermaphrodites exhibit nucleoli. The maternal effect of a single copy of *ncl-1(+)* in the hermaphrodite parent is dissipated by the time of hatching. Regardless of the genotype of the mother, the differences between nucleolar sizes in mutant and wild-type animals can be distinguished in first stage larvae (L1) and become more pronounced in later larvae (L3 and L4) and adults.

***ncl-1* genetic mosaics:** To explore the utility of *ncl-1* as a cell marker for mosaic analysis, we first used the free duplication *sDp3(III;f)* (ROSENBLUTH *et al.* 1985), which carries *ncl-1(+)* and which has been shown to be mitotically unstable (KENYON 1986). We constructed a strain of genotype *dpy-1 ncl-1; sDp3*[*dpy-1(+) ncl-1(+)*], picked L2-L4 non-Dpy animals, and inspected by Nomarski microscopy the sizes of the nucleoli of six neurons: ASKL, ADLL, ASIL, ASKR, ADLR and ASIR; these cells are easy to identify quickly and are not closely related (SULSTON *et al.* 1983; Figure 3). Nine percent (66/700) of the animals screened (reared at 20°) showed *ncl-1* mosaicism for one or more of the six neurons; examples are shown in Figure 6. When one or more of the cells of an animal were Ncl, we scored many lineally related cells (SULSTON *et al.* 1983) to see whether or not the pattern of mosaicism was consistent with the mitotic loss of the duplication by a single progenitor cell and the cell autonomy of *ncl-1*. Examples of mosaic expression of *ncl-1* in hypodermis and in body muscle are illustrated in Figure 7. In most cases, mosaic animals were explicable as "simple mosaics," in which *sDp3* was apparently lost by a single progenitor, as illustrated by the example in Figure 8. These simple mosaics also strongly support the view that *ncl-1* acts cell autonomously. Because many neighboring cells in the animal, even members of the same sensillum, are often distantly related by lineage, cells in *ncl-1* clones were typically surrounded by *ncl-1(+)*-containing cells.

In the example given in Figure 8, all of the indicated descendants of the cell ABpr were Ncl, with one signficant exception, and all other cells were non-Ncl. The exceptional cell fused early in development with a cell derived from ABpl to become the binucleate cell hyp10 (SULSTON *et al.* 1983). We conclude that when one of the two cells that fuse to form hyp10 is *ncl-1* and the other carries *ncl-1(+)*, then both nuclei become non-Ncl; the common cytoplasm must generate a product encoded by *ncl-1(+)* that acts on the mutant nucleus. We have seen many mosaic animals in which one of the two hyp10 nuclei must have been *ncl-1*, and only when both hyp10 nuclei were *ncl-1* did the two nuclei have enlarged nucleoli. In contrast, the hyp8 and hyp9 hypodermal cells are mononucleate, and they behaved cell autonomously in *ncl-1* mosaics.

At low frequency (in four mosaic animals out of a total of 66 mosaic animals), two unrelated mutant clones were found in the same animal; the frequency of these events was no higher than expected for independent events. In addition, however, we found animals in which *sDp3* was lost at two or three consecutive cell divisions. When two consecutive losses occur, the duplication is transmitted to only one daughter at consecutive divisions, with the consequence that an aunt and niece (and their descendants) are rendered homozygous mutant. We refer to such events as consecutive mosaics. The frequency of consecutive mosaics (7 compared to 93 simple mosaics) appeared to be higher than expected by chance; an example of a consecutive mosaic is given in Figure 9. (Two triple consecutive mosaics are described below in the section on mitotic nondisjunction of *sDp3*.) It is possible that a few of the mosaics we classified as simple might have suffered consecutive losses. To confirm that a putative simple mosaic is not consecutive it is necessary to show that

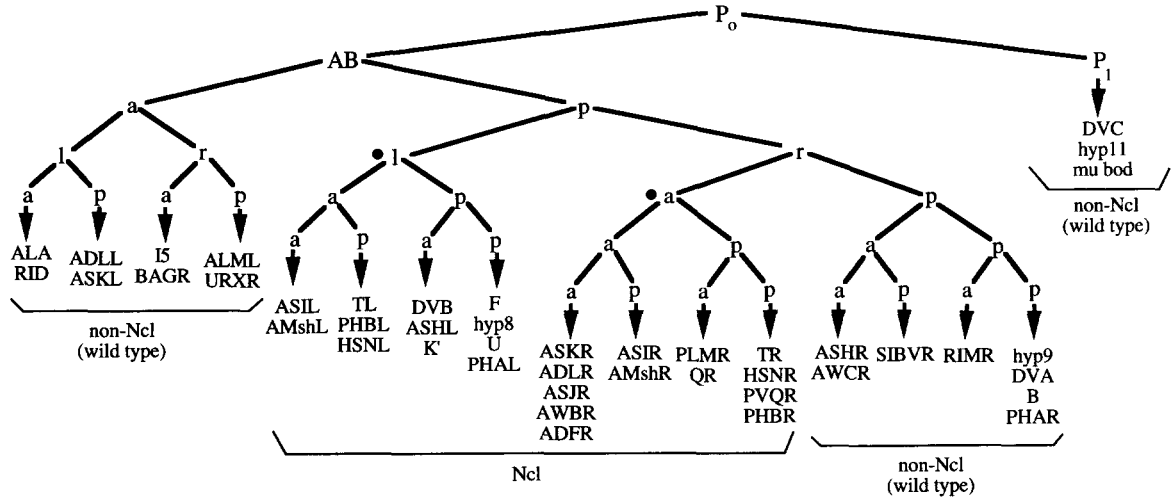

FIGURE 9.—Example of a consecutive mosaic. All of the descendants of one cell (ABpl) and one of its two nieces (ABpra) were Ncl.

descendants of all four granddaughters of the cell that lost the duplication are Ncl and that descendants of the aunt and two nieces of the cell that lost the duplication are non-Ncl. It is sometimes impossible to satisfy all of these criteria. Duplication loss may occur too late in the lineage for four granddaughters to be generated, or one or more of the relevant cells may not be scoreable (see below). Nonetheless, examples in which all criteria for a simple mosaic were satisfied (as in Figure 8) were much more frequent than were consecutive mosaics.

We carefully characterized 93 simple and 7 consecutive *dpy-1 ncl-1; sDp3* mosaics. The points in the lineage at which the duplication was lost in these 100 events are shown in Figure 10 (only the position of the first loss for each of the consecutive mosaics is shown). The results show that the probability of loss per cell division is approximately constant throughout the lineage that generates these six neurons. In some cases, shown by brackets in Figure 10, duplication loss could only be narrowed to a cell or its mother (or grandmother, in two cases), either because its sister (or aunt) had under-

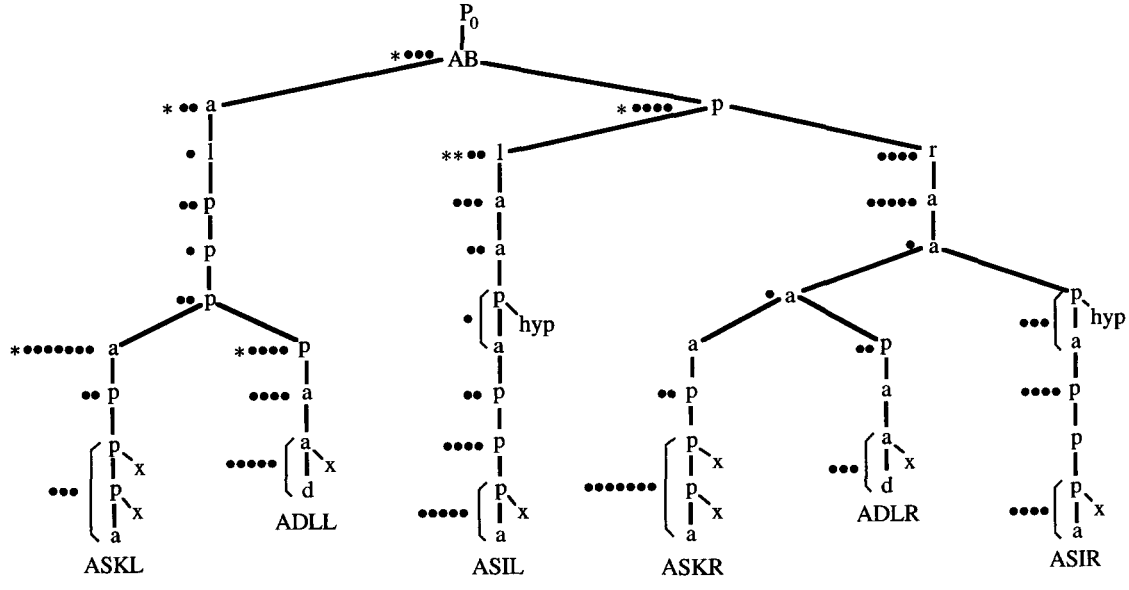

FIGURE 10.—Points in the cell lineage at which *sDp3* was lost; 100 events are shown. Non-Dpy *dpy-1 ncl-1; sDp3* animals were picked, and six neurons (ASKL, ADLL, ASIL, ASKR, ADLR and ASIR) were scored for the Ncl phenotype. For each mosaic animal found, many additional cells were scored, as illustrated by Figures 8 and 9, so that the position in the lineage at which the duplication was lost could be pinpointed. Each of the dots represents an event that appeared to be simple. The asterisks represent the position of the first duplication loss in a consecutive mosaic (the second losses for the consecutive mosaics are not shown). Brackets mark two or three consecutive cell divisions that cannot be distinguished, either because cells in the lineage (marked with an x) are absent owing to programmed cell death or because a cell in the lineage has fused with a hypodermal syncytium and will not exhibit a Ncl phenotype even if mutant.

TABLE 2

Frequencies of duplication loss

	Genotype	Temperature	No. of duplication losses/no. of cell divisions scored	Frequency of mitotic *Dp* loss per cell division ±95% confidence limits ($\times 10^3$)
1	*dpy-1 ncl-1; sDp3*	20°	76/33,234	2.3 ± 0.5
2	*dpy-1 ncl-1; sDp3*	20°	50/20,413	2.4 ± 0.7
3	*dpy-1 ncl-1; sDp3*	16°	41/20,876	2.0 ± 0.6
4	*dpy-1 ncl-1; sDp3*	24°	50/16,060	3.1 ± 0.9
5	*ncl-1 unc-36; sDp3*	20°	27/13,757	2.0 ± 0.8
6	*ncl-1 unc-36; qDp3*	20°	3/23,636	$0.1^{+0.3}_{-0.07}$
7	*ncl-1 unc-36; mnDp84*	20°	43/8,144	5.3 ± 1.6
8	*ncl-1 unc-36; mnDp86*	20°	39/8,892	4.4 ± 1.4
9	*ncl-1 unc-36; mnDp90*	20°	40/8,113	4.9 ± 1.6
10	*ncl-1 unc-36; mnDp89*	20°	16/18,697	0.9 ± 0.5
11	*dpy-1 ncl-1; unc-3 osm-1; mnDp91*	20°	5/12,998	$0.4^{+0.5}_{-0.3}$
12	*dpy-1 ncl-1; unc-3 osm-1; mnDp92*	20°	6/16,251	$0.4^{+0.4}_{-0.3}$
13	*dpy-1 ncl-1; sDp3; him-4*	20°	25/10,899	2.3 ± 0.9
14	*ncl-1 unc-36; mnDp90; him-8*	20°	34/6,395	5.3 ± 1.9
15	*him-10 ncl-1 unc-36; mnDp84*	20°	67/3,131	21 ± 5
16	*him-10 ncl-1 unc-36; mnDp84*	16°	46/4,524	10 ± 3
17	*him-10 ncl-1 unc-36; mnDp90*	20°	44/2,360	19 ± 6
18	*him-10 ncl-1 unc-36; mnDp89*	20°	41/6,152	6.7 ± 2.1
19	*dpy-1 him-10 ncl-1; unc-3 osm-1; mnDp91*	20°	24/10,523	2.3 ± 1.0
20	*dpy-1 him-10 ncl-1; unc-3 osm-1; mnDp92*	20°	17/6,883	2.5 ± 1.2
21	*him-10 ncl-1 unc-36; mnDp86[him-10(+)]*	20°	27/7,509	3.6 ± 1.4

gone programmed cell death or because its sister generated descendants that fused with *ncl-1(+)* cells to form hypodermal syncytia; as we have already indicated, all nuclei in hypodermal syncytia that contain both *ncl-1* and *ncl-1(+)* nuclei are non-Ncl.

Many duplication losses denoted in Figure 10 occurred during one of the last two (or three) cell divisions that gave rise to a terminally differentiated neuron. This means that *ncl-1(+)* must be active late, probably within the neuron itself; it may also be active during earlier periods of embryogenesis, but if so, the gene exhibits very little perdurance, *i.e.*, any *ncl-1(+)* gene product produced by ancestral cells does not persist sufficiently to prevent the appearance of enlarged nucleoli. This is perhaps not surprising in view of the fact that the neurons must generate dendrites and axons after they are born, about halfway through embryogenesis (SULSTON *et al.* 1983), and then increase in size during larval development.

Using *ncl-1* mosaics to measure frequencies of mitotic loss of a duplication: From the experiments described in the preceding section, we can estimate the frequency of *sDp3* loss per cell division, assuming an equal probability for all divisions. The six amphid neurons that were scored are generated by a total of 44 cell divisions. Thus, in non-mosaic animals, 44 cell divisions were negotiated by the duplication successfully. In mosaic animals, however, the number of divisions sampled is less because all divisions in a lineage following a point of duplication loss must be excluded from consideration (see MATERIALS AND METHODS). For a series in which we kept a careful tally of all animals scored, we found 76 losses in 33,234 cell divisions, or 2.3×10^{-3} per cell division, for animals reared at 20° (Table 2, line 1).

In order to measure frequencies of duplication loss more efficiently, we have scored the Ncl phenotype of 21 somatic cells chosen for their ease of scoring and disparate lineage; the 21 cells are generated by 140 cell divisions (Figure 3). In these experiments, additional cells were generally not scored and we did not attempt to locate the position of duplication loss precisely in the cell lineage (see MATERIALS AND METHODS for details on scoring). Results obtained by this method were in excellent agreement with our first procedure (Table 2, lines 1 and 2).

Table 2 (lines 2–4) shows that the frequency of mitotic loss of *sDp3* increased only mildly with increased growth temperature: the frequency of loss for animals reared at 24° was roughly 50% higher than for those reared at 16°.

Frequencies of mitotic loss of different duplications: The duplication *qDp3* (AUSTIN and KIMBLE 1987) also carries *ncl-1(+)*, although its endpoints are different from those of *sDp3* (Figure 2). The frequencies of loss of *sDp3* and *qDp3* were compared; *qDp3* does not carry *dpy-1(+)*, but both duplications carry *unc-36(+)*, so we put both duplications in the same genetic background, *ncl-1 unc-36*, for purposes of comparison. The

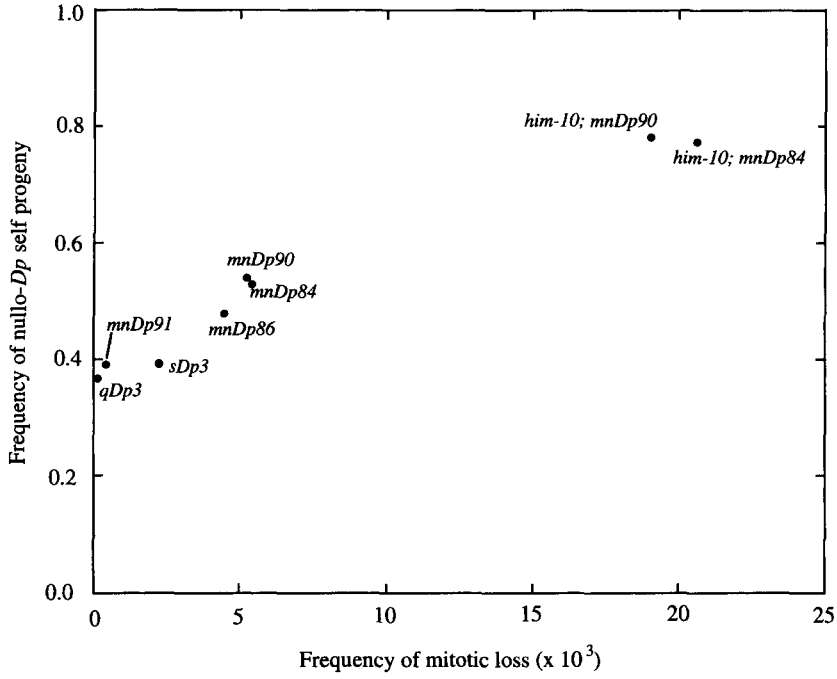

FIGURE 11.—Correlation between the frequency of mitotic duplication loss and the frequency of self-progeny that do not inherit a duplication.

frequency of mitotic loss of *qDp3* was only about 5% that of *sDp3* (Table 2, lines 5 and 6), despite the fact that the DNA content of *qDp3* appears to be less than that of *sDp3* (see DISCUSSION).

We have generated *ncl-1(+)*-bearing derivatives of *sDp3* that lack *sma-3(+)* and *lon-1(+)*, which map to the left of *ncl-1*. The derivatives were identified among exceptional Sma non-Unc progeny of *sma-3 ncl-1 unc-36; sDp3* hermaphrodites following gamma-ray treatment (see MATERIALS AND METHODS; Figure 2). The frequencies of mitotic loss of two of these duplications, *mnDp84* and *mnDp86*, were enhanced, roughly twofold, compared with *sDp3* (Table 2, lines 7 and 8). The free duplication *mnDp90* was generated as a spontaneous derivative of *mnDp86* that lacks *him-10(+)*; the frequency of mitotic loss of *mnDp90* (Table 2, line 9) was not much different from that of its progenitor, *mnDp86*.

Fusing a *ncl-1(+)*-bearing free duplication to unlinked free duplications: Because *ncl-1(+)* is an excellent cell marker for tracking duplication loss, it could be useful to tag unlinked duplications with it. We have accomplished this by fusing unlinked duplications to a *ncl-1(+)*-bearing duplication. To illustrate how this was done, consider a strain of genotype *dpy-1 ncl-1 III; sDp3(III;f); unc-3 osm-1 X; mnDp14(X;f)*. The two unlinked duplications segregate independently at meiosis, yielding all recombinant classes, including Dpy non-Unc and Unc non-Dpy animals. After treatment with gamma rays, wild-type animals were picked individually to fresh plates, and self-progeny broods were screened for the presence of wild-type and Dpy Unc progeny only. In this way, we made fusions of *sDp3* and *mnDp14(X;f)*, a fusion of *sDp3* and *mnDp30(X;f)*, fusions of *mnDp84* and *mnDp14*, and fusions of *mnDp90* and *mnDp14*. The fused duplications involving *sDp3* were extremely stable mitotically (data not shown), however, perhaps as a consequence of their large size. The duplication *mnDp89*, which was generated by the fusion of *mnDp84* and *mnDp14*, is considerably more stable that *mnDp84*, but it gives mosaic animals at a reasonable frequency (Table 2, line 10). Similarly, *mnDp91* and *mnDp92*, which were generated by fusions of *mnDp90* and *mnDp14*, are more stable than *mnDp90* (Table 2, lines 11 and 12). (For unknown reasons, males carrying *mnDp84* or *mnDp89* are infertile, whereas males carrying *mnDp90*, *mnDp91* or *mnDp92* are fertile.)

A *him-10* mutation markedly enhances mitotic duplication loss: We were interested in identifying mutations that enhance the frequency of mitotic duplication loss. Mutation in *him-4* leads to increased meiotic nondisjunction of the *X* chromosome and various other abnormalities (HODGKIN *et al.* 1979; E. HEDGECOCK, unpublished data) but had no discernable effect on the frequency of mitotic loss of *sDp3* (Table 2, line 13). A *him-8* mutation, which also increases meiotic nondisjunction of the *X* chromosome (HODGKIN *et al.* 1979), also had little effect on mitotic duplication loss (line 14). A *him-10* mutation, however, which affects mitotic chromosome segregation (A. VILLENEUVE, personal communication), markedly increased the frequency of mitotic loss of duplications (Table 2). The frequencies of loss of *mnDp84*, *mnDp89*, *mnDp90*, *mnDp91* and *mnDp92* were all increased about four- to sixfold for animals reared at 20° (Table 2, lines 15, 17–20). The *him-10* mutation is temperature sensitive with respect to its effects on both the incidence of male self-progeny and on fertility (HODGKIN *et al.* 1979), and it was only about half as effective at 16° as at 20° in promoting

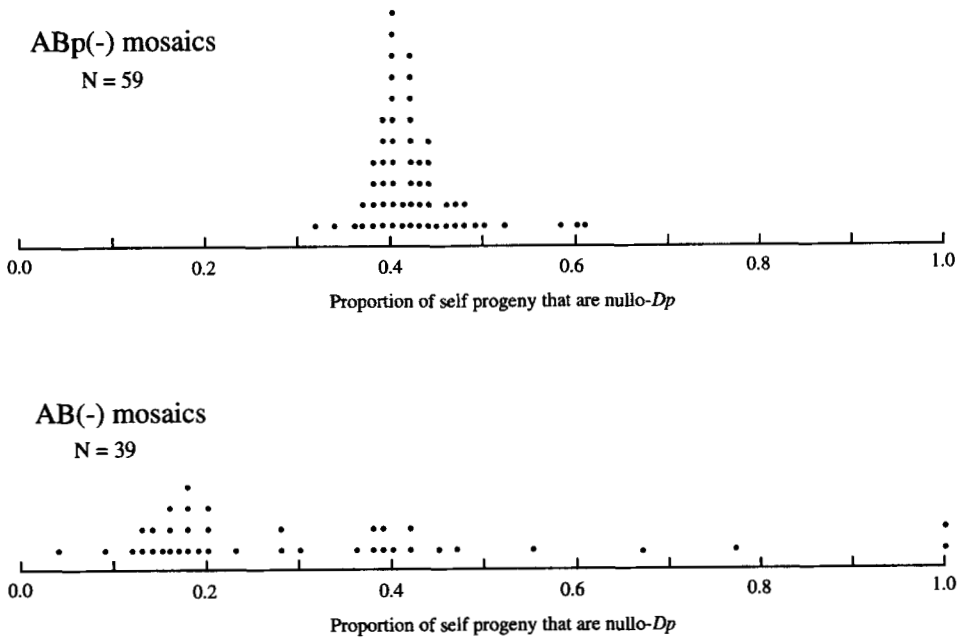

FIGURE 12.—Histograms showing the proportions of nullo-*sDp3* self-progeny produced by AB(−) and ABp(−) mosaics arising from *dpy-1 ncl-1 unc-36; sDp3* zygotes. Each dot represents one mosaic animal. Among the 59 ABp(−) mosiacs, the median frequency at which their single copy duplication was not transmitted to the next generation was 0.42. The expected median probability of two copies of the duplication not being transmitted to the next generation would be about 0.42 × 0.42 = 0.18, assuming that the two duplications behave independently. The smallest and median brood sizes were 70 and 225 for ABp(−) mosaics and 55 and 126 for AB(−) mosaics, respectively.

mitotic loss of *mnDp84* (Table 2, lines 15 and 16). Homozygous *him-10* stocks were essentially sterile at 25°. The duplication *mnDp86* carries *him-10(+)*, and this one copy was dominant to the two copies of *him-10(e1511*ts) carried by chromosomes *III*, both with respect to the frequency of duplication loss (Table 2, line 21) and the incidence of male self-progeny.

The frequency of mitotic duplication loss correlates with the frequency of self-progeny that fail to inherit the duplication: Different free duplications may exhibit different frequencies of transmission to self-progeny. The frequency at which self-progeny fail to inherit a duplication may reflect meiotic as well as mitotic duplication loss. It may also depend on the viability of animals carrying two copies per cell of a free duplication, since such animals would be expected to give fewer nullo-duplication self-progeny (see below); as will be shown in the next section, animals carrying two copies of *sDp3*, at least, are sickly and probably systematically excluded from the data of Figure 11. In any case, Figure 11 shows that there is an apparent correlation between the frequency of mitotic duplication loss and the proportion of self-progeny that fail to inherit the duplication, at least for this set of overlapping and mostly related duplications.

Mitotic nondisjunction of *sDp3*: We have asked whether or not mitotic duplication loss can occur as a consequence of duplication nondisjunction, in which case the sister of the cell that lost the duplication would receive two copies of the duplication. For these experiments, we identified AB(−) (duplication loss at AB) mosaics and then measured the duplication copy number of the mosaic animals' germlines, which are descended from P_1, the sister of AB (Figure 3). We measured the duplication copy numbers by two independent methods in two separate sets of experiments. In each case, we used animals of genotype *dpy-1 ncl-1 unc-36; sDp3* and screened for Unc non-Dpy segregants, which were then scored for mitotic duplication loss using the Ncl phenotype. KENYON (1986) previously showed that the anatomical focus of *unc-36* action is among the descendants of ABp(−); we show below that the focus of *dpy-1* action is diffusely distributed, apparently among hypodermal cells, which are derived from both AB and P_1. Most of the Unc non-Dpy animals, as a consequence, were either AB(−) or ABp(−) mosaics. To classify an animal as an AB(−) mosaic, we required that at least one descendant of each of the four granddaughters of AB be scored (and be Ncl) and that at least some descendants of P_1 be non-Ncl. We used the ABp(−) mosaics as controls, since their germlines should be unaffected.

In the first set of experiments, each mosaic animal was allowed to generate self-progeny, which generally included both nullo-*sDp3* (Dpy Unc) and *sDp3*-bearing (wild-type) animals. The proportion of nullo-*sDp3* progeny was measured for each mosaic animal. For the 59 ABp(−) mosaics that were scored, the median proportion of nullo-*sDp3* progeny was 0.42, with a range of 0.32 to 0.61 (Figure 12). We presume that the progenitor cell of the germlines of the ABp(−) mosaic animals contained a single copy of *sDp3*. If the germline progenitor of an AB(−) mosaic contained two copies of *sDp3*, we would expect a lower proportion of nullo-*sDp3* self-progeny. Indeed, among the 39 AB(−) mosaics scored, 24 gave a proportion of nullo-*sDp3* progeny of less than 0.3 (Figure 12). If we assume that two duplications would behave independently at meiosis—without pairing, for example—then the expected mean frequency of nullo-*sDp3* progeny would be 0.42 × 0.42 = 0.18, which was approximately the mean proportion of nullo-*sDp3* progeny for the 24 AB(−) mosaics with values

TABLE 3

Detection of free duplications by DAPI staining of oocytes

	Proportion of oocytes showing six bivalents plus the indicated number of fragments			
	0	1	2	>2
ABp(−) mosaics[a]	0.31 (34/110)	0.69 (76/110)	0.00 (0/110)	0.00 (0/110)
AB(−) mosaics[b]	0.16 (16/103)	0.56 (58/103)	0.28 (29/103)	0.00 (0/103)
Expected frequencies for two duplications[c]	0.10	0.43	0.48	0.00

[a] The total of 110 oocytes scored were found in 34 ABp(−) mosaic animals; the mean number of oocytes scored per animal and the sample standard deviation for oocytes scored per animal were 3.2 and 1.4, respectively.

[b] The total of 103 oocytes scored were found in 41 AB(−) mosaic animals; the mean number of oocytes scored per animal and the sample standard deviation for oocytes scored per animal were 2.5 and 1.1, respectively. Sixteen (39%) of the AB(−) mosaic animals had at least one occyte showing two fragments.

[c] The expected frequencies for 0, 1 and 2 fragments were calculated from the ABp(−) results as follows: 0.31×0.31, $2 \times 0.31 \times 0.69$ and 0.69×0.69, respectively.

under 0.3 (Figure 12). We therefore estimate that 24/39 or 62% of the AB(−) mosaics were generated by nondisjunction, in which two copies of *sDp3* were segregated to P_1. Most of the remaining 15 AB(−) mosaics appeared to involve simple duplication loss. In two cases, the germline of ABp(−) mosaics appeared to receive no duplication, because none of the self-progeny carried one (Figure 12). These two parents could have been consecutive mosaics, in which the duplication was lost at AB and P_2. Two of the Unc non-Dpy animals identified in this screen were in fact triple consecutive mosaics: each was P_1(−) ABa(−) ABpr(−). It seems very unlikely that the losses occurring in consecutive mosaics involve nondisjunction.

The AB(−) mosaics were smaller and less fertile on average than the ABp(−) mosaics. We suggest that two copies of *sDp3* in many cells of an animal's body may be deleterious. It was shown in earlier experiments that animals carrying two copies of another free duplication, *mnDp26*, are viable but retarded in their development and give small brood sizes compared to animals bearing a single copy of the duplication (HERMAN *et al.* 1979). We do not know if self-progeny of *sDp3*-bearing hermaphrodites carrying two copies of the duplication in essentially all somatic cells are viable, *i.e.*, we have made no attempt to estimate the incidence of two-duplication zygotes or progeny from *sDp3*-bearing animals. An advantage of using ABp(−) mosaics as controls is that their mosaicism makes it likely that they carried a single duplication as zygotes.

In the second set of experiments, AB(−) and ABp(−) mosaics were identified as before, but the animals were then stained with DAPI, and the oocytes were scored cytologically for the presence of small chromosome fragments in addition to the normal set of six bivalents. The oocytes of ABp(−) mosaics frequently exhibited a single chromosome fragment in addition to the normal set of six bivalents, and no cases of two fragments were found (Table 3). A relatively high proportion (31%) of the ABp(−) oocytes showed no fragment, a result that has been noted previously (HERMAN *et al.* 1976). The reason for this could be either that many oocytes contained no duplication, as a consequence of premeiotic duplication loss, or that the duplication contained in many oocytes was simply not observed, perhaps because it was situated too close to a bivalent. In any case, 28% of the scored oocytes in AB(−) mosaics showed two fragments (Table 3; Figure 13). If we assume that the two duplications behave independently, we would expect that about $0.69 \times 0.69 = 48\%$ of the oocytes of an animal in which the germline progenitor carried two duplications would show two detectable chromosome fragments. From the observed frequency of 28%, we conclude that about 58% (0.28/0.48) of the AB(−) mosaics were generated by nondisjunction, which is in very good agreement with the preceding estimate.

The focus of *dpy-1* function is in hypodermis: Loss of *dpy-1(+)* from all AB cells in an otherwise *dpy-1 ncl-1 unc-36; sDp3* animal does not result in an overall Dpy body shape. Furthermore, the two triple mosaic animals referred to above in which *dpy-1(+)* was lost by P_1, ABa and ABpr were also essentially non-Dpy. Additional P_1(−) *dpy-1* mosaics, which were non-Dpy, are described below. We conclude that the focus of *dpy-1* expression with respect to overall Dpy body shape must be diffuse; expression of *dpy-1(+)* among descendants of P_1 or AB (or ABpl) must be sufficient to give a non-Dpy body shape. This conclusion is supported by our inability to

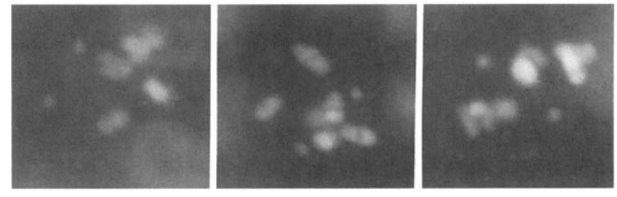

FIGURE 13.—Photomicrographs of DAPI-stained oocytes of AB(−) mosaics showing the presence of two copies of *sDp3*. The oocytes were not squashed, so the six chromosome bivalents are not all in the same plane of focus. Magnifications: ×1600.

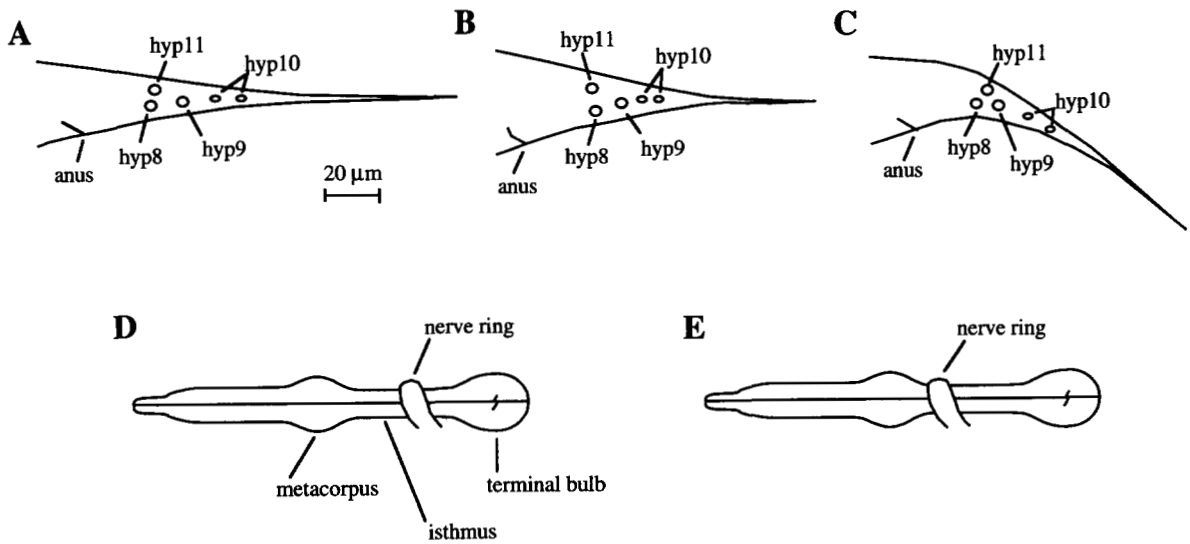

FIGURE 14.—Drawings, based on drawings made with a Zeiss 45° drawing prism, of animals mounted on agar pads to illustrate the effects of *dpy-1* mosaicism on tail bending and nerve ring positioning. All animals are mid-L4 larvae. Anterior is to the left and dorsal is up. (A) Wild-type tail of a *dpy-1 ncl-1 unc-36; sDp3* animal. Nuclei of tail hypodermal cells are shown. (B) Dpy tail of a *dpy-1 ncl-1 unc-36* animal. (C) Ventral tail bend of an ABp(−) mosaic arising from a *dpy-1 ncl-1 unc-36; sDp3* zygote. (D) Position of nerve ring in a *dpy-1 ncl-1 unc-36; sDp3* non-Dpy animal. (E) Position of nerve ring in *dpy-1 ncl-1 unc-36* animals and AB(−) mosaics arising from *dpy-1 ncl-1 unc-36; sDp3* zygotes. Similar results for tail bends and nerve ring positions were found for mosaics arising from *dpy-1 ncl-1; sDp3* zygotes. The magnifications of all drawings, indicated in A, are identical.

find *dpy-1 ncl-1 unc-36; sDp3* mosaics with a Dpy non-Unc phenotype. The most likely interpretation of these results is that the overall Dpy body shape is a consequence of the lack of *dpy-1(+)* expression in the hyp7 syncytial hypodermis, which covers much of the body; hyp7 nuclei arise from descendants of ABa, ABpl, ABpr and P_1 (SULSTON *et al.* 1983).

We have discovered anatomical abnormalities in the heads and tails of particular *dpy-1* mosaics, which we also attribute to hypodermal *dpy-1* expression. Animals homozygous for *dpy-1* have stubby tails (Figure 14). The AB(−) and ABp(−) mosaics described in the previous section invariably displayed a sharp ventral bend in their tails (Figure 14). We confirmed the idea that these bends were due to the absence of *dpy-1(+)* among descendants of ABp (and not an effect of *unc-36*) by identifying six *dpy-1 ncl-1; sDp3* animals with ventral tail bends; using the Ncl phenotype, we showed that three of these animals were AB(−) mosaics and that the other three were ABp(−) mosaics. The ventral tail bend is thus a useful diagnostic for identifying AB(−) and ABp(−) mosaics arising from *dpy-1 ncl-1; sDp3* zygotes. We propose that the ventral tail bend of AB(−) and ABp(−) mosaics is caused by both the absence of *dpy-1(+)* from the mononucleate ventral tail hypodermal cells hyp8 and hyp9, which descend from ABpl and ABpr, and the presence of *dpy-1(+)* in the dorsal tail hypodermal cell hyp11, which descends from P_1. A shortening of hyp8 and hyp9 without concomitant shortening of hyp11 would be expected to lead to a ventral tail bend. The *dpy-1* genotype in AB(−) and ABp(−) mosaics of the most posterior hypodermal cell, the binucleate cell hyp10, may also contribute to the ventral tail bend. Some P_1(−) *dpy-1* mosaics (see next section), in which hyp11 is *dpy-1* and other tail hypodermal cells are *dpy-1(+)*, exhibited a weak dorsal tail bend, but we have not been able to identify *dpy-1* hyp11 mosaics reliably on the basis of a dorsal tail bend.

The abnormality in the head that we have correlated with *dpy-1* mosaicism concerns the position of the nerve ring in relation to the pharynx. In wild-type animals, the nerve ring nearly surrounds (on all but the ventral side) the isthmus of the pharynx at a position, in larvae, about halfway between the metacorpus and terminal bulb (Figure 14). (In older adults, the nerve ring becomes relatively closer to the terminal bulb, although still on the isthmus.) In *dpy-1* animals, the nerve ring is more anteriorly situated; it is around the isthmus at a position almost adjacent to the metacorpus (Figure 14). We measured the nerve ring positions in 14 AB(−) and 11 ABp(−) mosaics arising from *dpy-1 ncl-1 unc-36; sDp3* zygotes; the mosaic animals were identified in our analysis of mitotic nondisjunction of *sDp3*. The nerve rings of all of the AB(−) mosaics were at the anterior position characteristic of *dpy-1* animals, whereas the nerve rings of all of the ABp(−) animals were more medially situated, at about the same position as is found for non-mosaic *dpy-1 ncl-1 unc-36; sDp3* animals. This effect is unrelated to the *unc-36* gene; three AB(−) mosaics arising from *dpy-1 ncl-1; sDp3* zygotes, identified on the basis of ventral tail bends, had their nerve rings at the anterior position.

We interpret the effect of *dpy-1* mosaicism on the position of the nerve ring as an effect on the anterior

hypodermal cells hyp4, hyp5 and hyp6. One of the three hyp4 nuclei, one of the two hyp5 nuclei and two of the six hyp6 nuclei descend from ABa; the others all descend from ABp (SULSTON *et al.* 1983). We suggest that when all of the hyp4, hyp5 and hyp6 nuclei are *dpy-1,* the cells are shortened and the nerve ring is situated more anteriorly as a consequence. We have in fact noted that the positions of the hyp6 nuclei and neighboring hyp7 nuclei are more anteriorly situated in *dpy-1* and AB(−) mosaics than in wild-type animals. We thus suggest that the position of the nerve ring is determined by the position of surrounding hypodermis.

The action of *lin-37* on vulva development is cell nonautonomous: Mutations in *lin-37 III* are synthetic Muv class B, and *lin-8 II* mutations are synthetic Muv class A. Consider animals of genotype *lin-8 II; dpy-1 lin-37 ncl-1 unc-36; sDp3*[*dpy-1(+) lin-37(+) ncl-1(+) unc-36(+)*]. Among 100 Dpy Unc self-progeny of these animals, 93 were clearly Muv, exhibiting at least one pseudovulva anterior or posterior to the normal vulva. It is possible that the *dpy-1* mutation suppresses very slightly the appearance of pseudovulvae: 98 of 100 Unc-36 segregants of *lin-8 II; lin-37 ncl-1 unc-36; sDp3* animals were Muv. We scored 2,237 non-Dpy non-Unc self-progeny of the *lin-8; dpy-1 lin-37 ncl-1 unc-36; sDp3* animals and found that none was Muv as a consequence of duplication loss (one Muv animal proved to be the result of duplication breakdown, since its progeny were all Muv). Next, we picked rare Unc non-Dpy animals and scored many cells in each with respect to the Ncl phenotype in order to identify AB(−) and ABp(−) mosaics. All six vulval precursor cells derive from AB.p, so if *lin-37* is cell autonomous in its action, we would expect both AB(−) and ABp(−) mosaics to be Muv. We found, however, that among 23 AB(−) mosaics, only 3 were Muv, and among 24 ABp(−) mosaics, none was Muv. We conclude that *lin-37* is acting cell nonautonomously and that its focus of action is not limited to descendants of AB.

To identify *lin-37* $P_1(-)$ mosaics, we constructed animals of genotype *lin-8 II; dpy-1 unc-93(0) lin-37 ncl-1 unc-36 III; sDp3(III;f); sup-10(n983) X.* The *sup-10(n983)* mutation confers a phenotype of uncoordination referred to as rubberband (GREENWALD and HORVITZ 1986), the focus of which is in body muscle (VILLENEUVE and MEYER 1990). The rubberband phenotype is recessively suppressed by null mutations in *unc-93,* referred to as *unc-93(0),* which by themselves have a wild-type phenotype. The *sDp3*-bearing animals are not suppressed because *sDp3* carries the dominant *unc-93(+)* allele; they are non-Dpy non-Unc-36 non-Muv rubberband. The nullo-duplication self-progeny are Dpy Unc-36 non-rubberband; and among 100 such animals, 98 were Muv. $P_1(-)$ mosaics are suppressed for the rubberband phenotype because all body wall muscles but one descend from P_1 and are also non-Dpy and non-Unc-36 because the descendants of AB carry *dpy-1(+)* and *unc-36(+).* Rare non-Dpy non-Unc-36 non-rubberband segregants from the *sDp3*-bearing parents were thus sought, and the pattern of *ncl-1* mosaicism was then investigated to confirm $P_1(-)$ mosaics. As expected, all of the $P_1(-)$ mosaics segregated only nullo-*sDp3* self-progeny. We identified seven $P_1(-)$ mosaics and all were non-Muv.

DISCUSSION

Our interest in *ncl-1* in this work stemmed from its virtues as a cell autonomous marker for mosaic analysis, and we have done little to explore the nature of the *ncl-1* function that affects nucleolar size. Both mutant alleles are recessive to *ncl-1(+),* and *ncl-1/Df* exhibits the same phenotype as homozygous *ncl-1,* which suggests that the *ncl-1* mutations are loss of function. The cell autonomous action of *ncl-1* implies that wild-type gene product is retained within the cell of origin. We have also seen that when a cell contains a *ncl-1* nucleus and a *ncl-1(+)*-containing nucleus in the same cytoplasm, both nuclei have wild-type nucleoli. A plausible hypothesis is that the *ncl-1(+)* gene encodes a protein that is a negative regulator of ribosomal RNA synthesis.

Virtues of *ncl-1* for mosaic analysis: The *ncl-1* gene has five properties that recommend it as a cell marker for identifying the genotypes of different cells in mosaic animals. First, it is cell autonomous. Second, the Ncl phenotype can be scored in nearly every cell. Third, the phenotype can be scored in living animals of various ages. Fourth, mutation in *ncl-1* seems to have no discernable effect beyond enlarging nucleoli, which means that it does not affect the scoring of other mutant phenotypes. And finally, *ncl-1(+)* exhibits very little perdurance, so that losses very late in the cell lineage are readily detected. Indeed, *ncl-1* has already been exploited as a cell marker in the mosaic analysis of several other genes, including *glp-1* (AUSTIN and KIMBLE 1987), *lin-12* (SEYDOUX and GREENWALD 1989; SEYDOUX *et al.* 1990), *tra-1* and *her-1* (HUNTER and WOOD 1990, 1992), *pal-1* (WARING and KENYON 1991), various lethal mutations (BUCHER and GREENWALD 1991), *unc-5* (LEUNG-HAGESTEIJN *et al.* 1992), *mpk-1* (LACKNER *et al.* 1994) and *let-23* and *lin-7* (SIMSKE and KIM 1995).

Extending the applicability of *ncl-1* as a cell autonomous marker to the mosaic analysis of unlinked genes: Three approaches have been taken to the problem of extending the applicability of *ncl-1* as a cell marker to the mosaic analysis of unlinked genes that are not normally found on the same free duplication as *ncl-1.* Two of these approaches require the cloning of the gene to be analyzed. In an application of the first approach, LEUNG-HAGESTEIJN *et al.* (1992) injected a cosmid clone containing *unc-5(+),* the gene they wanted to analyze in mosaics, into the germline of *unc-5* hermaphrodites and recovered transformed animals carrying a transgenic extrachromosomal multi-gene array (FIRE 1986;

MELLO *et al.* 1991). Such extrachromosomal arrays are transmitted during mitosis and meiosis much like a free duplication, generally as one array per cell (STINCHCOMB *et al.* 1985). Next, gamma rays were used to stimulate the fusion of the array to *sDp3[ncl-1(+)]*. The altered free duplication, carrying both *unc-5(+)* and *ncl-1(+)*, was then used to conduct a mosaic analysis of *unc-5*. In the second approach (LACKNER *et al.* 1994; L. MILLER, D. WARING and S. KIM, personal communication), the germline is injected with DNA containing the gene of interest, a cosmid carrying *ncl-1(+)* and at least one additional gene that complements a visible marker; an extrachromosomal multicopy array carrying all three genes is formed (FIRE 1986; MELLO *et al.* 1991). The array is maintained in a strain that is otherwise homozygous mutant for *ncl-1*, the gene of interest and the visible marker and is then treated in the mosaic analysis as if it were a free duplication. This approach was used by LACKNER *et al.* (1994) to analyze *mpk-1* in mosaics and by SIMSKE and KIM (1995) to analyze *let-23* and *lin-7*.

There are potential problems with using extrachromosomal arrays for mosaic analysis. The expression of transgenes has frequently been shown to vary from animal to animal, and the variability seems not to be attributable solely to somatic duplication loss (KRAUSE *et al.* 1994; C. MELLO and A. FIRE, personal communication). In addition, transgenes are sometimes expressed in inappropriate tissues, apparently as a consequence of being driven by inappropriate promoters or of lacking negative regulatory sequences. Extrachromosomal arrays may also introduce unexpected dominance effects, which apparently can result from a variety of causes (C. MELLO and A. FIRE, personal communication). These potential problems are array-specific, which means that they should be assessed for each extrachromosomal array used in mosaic analysis.

The third approach to extending the applicability of *ncl-1* to the analysis of other genes is illustrated in this paper and involves the fusion of two unlinked free duplications, one carrying *ncl-1(+)* and the other carrying the gene to be analyzed. This method was used by HUNTER and WOOD (1992) in their mosaic analysis of *her-1*. We found it straightforward to generate fused duplications. The main difficulty is that the fused duplications tend to be considerably more stable mitotically than either of the original duplications alone, perhaps owing to their larger size. We have ameliorated this problem somewhat by generating a *ncl-1(+)*-containing duplication, *mnDp90*, which is fairly unstable mitotically and which seems to give less stable fusion products than the larger *ncl-1(+)*-containing duplication *sDp3*. We have also found that the fused duplications can be made less stable by using a *him-10* genetic background.

Factors affecting the mitotic stability of free duplications: KENYON (1987) estimated that *sDp3* was lost in approximately 1 in 400 cell divisions at 20° in *him-5* males; this agrees well with our measurements, conducted in different genetic backgrounds, and suggests that the *him-5* mutation has little effect on the frequency of duplication loss. BUCHER and GREENWALD (1991) found that *qDp3* was lost at a frequency less than about 10^{-4} per cell division, which is consistent with our estimate for a different genetic background. The factor of 20 or more difference in the frequencies of somatic loss of *qDp3* and *sDp3* is surprising because *qDp3* does not appear to be much larger than *sDp3*. The extent of *qDp3* on the physical map has been determined by *in situ* hybridization of YAC clones to *qDp3* and corresponds to about 4.5 Mb (D. ALBERTSON, personal communication). The endpoints of *sDp3* on the physical map are less well defined, but its size has been estimated at 5.5–7 Mb (D. ALBERTSON, personal communication). In agreement with these estimates, *sDp3* seems to carry about one-third more genes on the genetic map than does *qDp3*. Since the relative stabilities of *sDp3* and *qDp3* do not seem to be related to their size differences, it appears that some difference in DNA sequence or perhaps in duplication structure, such as linear *vs.* circular, accounts for the large difference in their mitotic stabilities.

Duplication size does seem to be an important factor in determining mitotic stability of duplications, however. The two pruned derivatives of *sDp3* were significantly less stable than *sDp3*, and each of more than a dozen fused derivatives we studied was more stable than either of its two progenitor duplications.

We found that duplications which exhibited high-frequency mitotic loss tended to be passed on to their self-progeny, and hence gametes, at low frequency (Figure 11). Some nullo-*Dp* gametes are formed as a consequence of meiotic segregation, but mitotic germline losses and meiotic losses may also occur; and it is difficult to determine the relative importance of each of these processes. HUNTER and WOOD (1990) noted for four different duplications that higher frequencies of germline transmission were correlated with increased mitotic stability. But one of their duplications, *ctDp2*, would be a severe outlier if placed on our Figure 11; its frequency of germline transmission was much lower than would be expected for its frequency of mitotic loss. We therefore suspect that the mitotic stability of a duplication cannot always be predicted from its germline transmission frequency.

A. VILLENEUVE (personal communication) observed abnormal chromosome numbers in the oocytes of *him-10* hermaphrodites and suggested that *him-10* causes defects in chromosome segregation in the mitotic germline. We were thus interested to see that *him-10* increases the frequency of mitotic loss of duplications approximately fivefold. The *him-10* gene appears to provide an essential function: *him-10(e1511)* is temperature sensitive and leads to sterility at 25°. In yeast, temperature-sensitive mutations in several genes that play roles in the cell division cycle have been shown to promote

mitotic chromosome loss (HARTWELL and SMITH 1985); furthermore, minichromosomes are more sensitive to mitotic loss in these mutants than are the normal yeast chromosomes (PALMER *et al.* 1990). It might be useful to search for new mutations in *C. elegans* that enhance mitotic loss of duplications; such mutations might define genes involved in controlling the cell division cycle. Enhanced loss of the duplication *mnDp90* can be detected after scoring just a few animals for *ncl-1* mosaicism.

Two other *him* mutations, in *him-4* and *him-8,* had no detectable effect on the frequency of mitotic loss. These mutations lead to enhanced formation of nullo-*X* gametes through *X* chromosome nondisjunction (HODGKIN *et al.* 1979), but their effects seem to be meoisis-specific.

Nature of mitotic loss of free duplications: The frequency of mitotic loss of *sDp3* ($\sim 10^{-3}$ per cell division) and most other free duplications appears to be much higher than for normal chromosomes. Examining the transmission behavior of *sDp3* during the first embryonic division, we observed two different patterns of duplication loss. In about 60% of the losses, one daughter cell received two copies of the duplication while its sister cell received none. In the remaining 40%, one daughter received a single copy while its sister received none. These patterns correspond to mitotic nondisjunction (2:0 segregation) and chromosome loss (1:0 segregation), respectively, described for normal chromosomes in other species (*e.g.*, GERRING *et al.* 1990).

ALBERTSON and THOMSON (1982) stained *C. elegans* chromosomes during early embryogenesis and observed that small free duplications often lie at the outer edge of the plate at metaphase and may lag behind the normal chromosomes at anaphase. They suggested that a paucity of microtubule attachment sites on these small chromosomes might reduce the fidelity of bipolar orientation and centration on the mitotic spindle. Such errors might account for both classes of events observed in *sDp3:* unipolar attachment to the spindle might result in nondisjunction, while improper centration or delayed chromosome separation might result in frank loss of lagging chromosomes during reformation of the nucleus at telophase. While our explanation presumes that free duplications replicate and condense on schedule with normal chromosomes, these segregation defects could be secondary to a delay or failure of replication.

An unexpected feature of mitotic chromosome loss in *C. elegans* is that many events involve loss of a free duplication at two or more consecutive cell divisions. A simple explanation is that the duplication becomes temporarily sequestered, say in the cytoplasm, at telophase. While sequestered, the duplication cannot replicate with the normal chromosomes. At the next mitosis, or even one later, the sequestered chromosome may recover spontaneously if it is recaptured by either the mitotic spindle itself or within the newly reformed nucleus of a daughter cell.

The *dpy-1* gene acts in hypodermis: We have concluded that the focus of *dpy-1* function with respect to overall body shape is in hyp7, the syncytial hypodermis that covers most of the body. The many cells that fuse to form hyp7 are derived from both AB and P_1 (SULSTON *et al.* 1983), which explains why neither AB(−) mosaics nor P_1(−) mosaics are Dpy. Three other *dpy* genes have been analyzed in mosaics; the foci of all three have been suggested to be in hypodermis, but the descendants of P_1 appear to be more important for *dpy-17* (KENYON 1986; YUAN and HORVITZ 1990) and *dpy-18* (HUNTER and WOOD 1990) function, whereas AB descendants seem more important for *dpy-4* (YUAN and HORVITZ 1990). Although none of the four *dpy* genes that have now been analyzed in mosaics has been cloned, other *dpy* genes have been shown to encode cuticle collagens that are presumably secreted by the hypodermis (for reviews, see JOHNSTONE 1994; KRAMER 1994).

We have uncovered specific defects in mosaics that we attribute to *dpy-1* expression in hypodermal cells of the head and tail. The head hypodermal cells anterior to hyp7 contain nuclei derived from both ABa and ABp (SULSTON *et al.* 1983), and we have found that these nuclei are more anteriorly situated relative to the pharynx in AB(−) mosaics, as if the *dpy-1* mutation leads to a shortening of the anterior hypodermal cells. We have found that the nerve ring in these animals is also more anteriorly situated in relation to the pharynx, which it surrounds. We therefore suggest that the positioning of the nerve ring during development depends upon the positioning of the overlying hypodermis. In the tail of the animal, we found that both AB(−) and ABp(−) mosaics display a ventral tail bend. We attribute this to the fact that the ventral hypodermal cells in the tail, hyp8 and hyp9 (as well as the most posterior hyp10), derive from ABpl and ABpr, whereas the dorsal tail hypodermal cell hyp11 derives from P_1. We thus propose that the ventral tail bend is due to a shortening of hyp8 and hyp9 on the ventral side (as well as hyp10 more posteriorly) in the absence of concomitant shortening of hyp11 on the dorsal side.

The silent Muv gene *lin-37* is cell nonautonomous and probably acts in hyp7: The *lin-37* mutation we have analyzed in mosaic animals is a class B synthetic Muv mutation. It results in a multivulva phenotype when present with a class A synthetic Muv mutation, such as the *lin-8* mutation used in our experiments (FERGUSON and HORVITZ 1989). The synthetic Muv genes have a maternal effect; FERGUSON and HORVITZ (1989) found that at 20° only about 44% of the *lin-8; lin-37* self-progeny of a *lin-8/+; lin-37/+* hermaphrodite were Muv, but 100% of the *lin-8; lin-37* progeny were Muv when the hermaphrodite parent was homozygous mutant at both loci. The strains used in our experiments were homozygous for *lin-8* and *lin-37* except for a single copy of *lin-37(+)* on

sDp3. Over 90% of the *lin-8; lin-37* self-progeny were Muv. None of the 24 ABp(−) mosaics was Muv, and because all of the vulval precursor cells (VPCs) are descended from ABp, we conclude that *lin-37* acts cell nonautonomously. In addition, none of seven P_1(−) mosaics was Muv, and only 3 of 23 AB(−) mosaics was Muv. We interpret these results by proposing that the focus of *lin-37* action is in hyp7, which is formed by the fusion of cells descended from ABa, ABp and P_1 (SULSTON *et al.* 1983). We further propose that the loss of *lin-37(+)* from the hyp7 nuclei descended from either ABp or P_1 does not reduce *lin-37(+)* expression sufficiently to lead to a mutant phenotype and that the loss of *lin-37(+)* by all AB-derived nuclei is only rarely sufficient, *i.e.*, that the *lin-37(+)* nuclei in the heterokaryonic hyp7 syncytium provide sufficient wild-type function.

A formal alternative interpretation would be that *lin-37(+)* must be expressed by the zygote nucleus P_0 and that loss of the duplication by either daughter of P_0 (AB or P_1) would occur too late to prevent wild-type function. This seems very unlikely, particularly because very little if any embryonic transcription occurs at this stage (EDGAR *et al.* 1994). We also emphasize that *lin-37(+)* expression in the oocyte cannot explain the non-Muv phenotype of the mosaic animals; many oocytes destined to produce Muv animals lose a free duplication via meiotic segregation only after fertilization, because the first meiotic division does not occur until then (HIRSH *et al.* 1976).

Our proposal for the focus of action of *lin-37* is identical to our earlier proposal for the Muv gene *lin-15* (HERMAN and HEDGECOCK 1990). For *lin-15* we found that ABpl(−), ABpr(−) and P_1(−) mosaics were sometimes partially Muv and suggested that *lin-15(+)* function in hyp7 had been reduced sufficiently in some of these mosaics to cause a partially mutant phenotype. In light of what we now know about mitotic nondisjunction, we would expect that some of the P_1(−) mosaics would transmit two copies of *lin-15(+)* to AB, in which case loss of the gene in the P_1-derived hyp7 nuclei might be compensated by increased copy number in the AB-derived nuclei; these mosaics might then be more likely to be the non-Muv ones. It appears that *lin-37(+)* is normally provided in greater excess than is *lin-15(+)* with respect to vulval function since fewer mosaic animals were Muv in the case of *lin-37*.

We thank NICHOL THOMSON for his able technical help with electron microscopy, CYNTHIA KENYON for her identification of *ncl-1(e1942)*, ANDY FIRE for getting us to think about fusing duplications, and CLAIRE KARI for her able help in pruning and fusing duplications. Some of the strains used were obtained from the Caenorhabditis Genetics Center, which is supported by the National Institutes of Health (NIH) National Center for Research Resources. This work was supported by NIH research grants NS-26295 (E.M.H.) and GM-22387 (R.K.H.).

LITERATURE CITED

ALBERTSON, D. G., and J. N. THOMSON, 1976 The pharynx of *Caenorhabditis elegans*. Philos. Trans. R. Soc. Lond. B Biol. Sci. **275:** 299–325.

ALBERTSON, D. G., and J. N. THOMSON, 1982 The kinetochores of *Caenorhabditis elegans*. Chromosoma **86:** 409–428.

ALBERTSON, D. G., and J. N. THOMSON, 1993 Segregation of holocentric chromosomes at meiosis in the nematode, *Caenorhabditis elegans*. Chromos. Res. **1:** 15–26.

AUSTIN, J., and J. KIMBLE, 1987 *glp-1* is required in the germ line for regulation of the decision between mitosis and meiosis in C. elegans. *Cell* **51:** 589–599.

AUSTIN, J., and J. KIMBLE, 1989 Transcript analysis of *glp-1* and *lin-12*, homologous genes required for cell interactions during development of C. elegans. Cell **58:** 565–571.

BRENNER, S., 1974 The genetics of *Caenorhabditis elegans*. Genetics **77:** 71–94.

BUCHER, E. A., and I. GREENWALD, 1991 A genetic mosaic screen of essential zygotic genes in *Caenorhabditis elegans*. Genetics **128:** 281–292.

CLARK, S. G., X. LU and H. R. HORVITZ, 1994 The *Caenorhabditis elegans* locus *lin-15*, a negative regulator of a tyrosine kinase signaling pathway, encodes two different proteins. Genetics **137:** 987–997.

CHALFIE, M., and J. SULSTON, 1981 Developmental genetics of the mechanosensory neurons of *Caenorhabditis elegans*. Dev. Biol. **82:** 358–370.

EDGAR, L. G., N. WOLF and W. B. WOOD, 1994 Early transcription in *Caenorhabditis elegans* embryos. Development **120:** 443–451.

ELLIS, H. M., and H. R. HORVITZ, 1986 Genetic control of programmed cell death in the nematode Caenorhabditis elegans. Cell **44:** 817–829.

FERGUSON, E. L., and H. R. HORVITZ, 1985 Identification and characterization of 22 genes that affect the vulval cell lineages of the nematode *Caenorhabditis elegans*. Genetics **110:** 17–72.

FERGUSON, E. L., and H. R. HORVITZ, 1989 The multivulva phenotype of certain *Caenorhabditis elegans* mutants results from defects in two functionally redundant pathways. Genetics **123:** 109–121.

FERGUSON, E. L., P. W. STERNBERG and H. R. HORVITZ, 1987 A genetic pathway for the specification of the vulval cell lineages of *Caenorhabditis elegans*. Nature **326:** 259–267.

FIRE, A., 1986 Integrative transformation of *Caenorhabditis elegans*. EMBO J. **5:** 2673–2680.

GARCIA-BELLIDO, A., and J. R. MERRIAM, 1971 Genetic analysis of cell heredity in imaginal discs of *Drosophila melanogaster*. Proc. Natl. Acad. Sci. USA **68:** 2222–2226.

GERRING, S. L., F. SPENCER and P. HIETER, 1990 The *CHL1 (CTF1)* gene product of *Saccharomyces cerevisiae* is important for chromosome transmission and normal cell cycle progression in G2/M. EMBO J. **9:** 4347–4358.

GREENWALD, I. S., and H. R. HORVITZ, 1986 A visible allele of the muscle gene *sup-10 X* of *Caenorhabditis elegans*. Genetics **113:** 63–72.

HARTWELL, L. H., and D. SMITH, 1985 Altered fidelity of mitotic chromosome transmission in cell cycle mutants of *S. cerevisiae*. Genetics **110:** 381–395.

HERMAN, R. K., 1984 Analysis of genetic mosaics of the nematode *Caenorhabditis elegans*. Genetics **106:** 165–180.

HERMAN, R. K., 1989 Mosaic analysis in the nematode *Caenorhabditis elegans*. J. Neurogenet. **5:** 1–24.

HERMAN, R. K., and E. M. HEDGECOCK, 1990 Limitation of the size of the vulval primordium of *Caenorhabditis elegans* by *lin-15* expression in surrounding hypodermis. Nature **348:** 169–171.

HERMAN, R. K., D. G. ABERTSON and S. BRENNER, 1976 Chromosome rearrangements in *Caenorhabditis elegans*. Genetics **83:** 91–105.

HERMAN, R. K., J. E. MADL and C. K. KARI, 1979 Duplications in *Caenorhabditis elegans*. Genetics **92:** 419–435.

HIRSH, D., D. OPPENHEIM and M. KLASS, 1976 Development of the reproductive system of *Caenorhabditis elegans*. Dev. Biol. **49:** 200–219.

HODGKIN, J., H. R. HORVITZ and S. BRENNER, 1979 Nondisjunction mutants of the nematode *Caenorhabditis elegans*. Genetics **91:** 67–94.

HODGKIN, J., M. EDGLEY, D. L. RIDDLE and D. G. ALBERTSON, 1988 Genetics, pp. 491–584 in *The Nematode Caenorhabditis elegans*, edited by W. B. WOOD. Cold Spring Harbor Laboratory, Cold Spring Harbor, NY.

HORVITZ, H. R., and P. W. STERNBERG, 1991 Multiple intercellular signaling systems control the development of the *Caenorhabditis elegans* vulva. Nature **351:** 535–541.

HORVITZ, H. R., S. BRENNER, J. HODGKIN and R. K. HERMAN, 1979 A uniform genetic nomenclature for the nematode *Caenorhabditis elegans*. Mol. Gen. Genet. **175:** 129–133.

HUANG, L. S., P. TZOU and P. W. STERNBERG, 1994 The *lin-15* locus encodes two negative regulators of *Caenorhabditis elegans* vulval development. Mol. Biol. Cell **54:** 395–411.

HUNTER, C. P., and W. B. WOOD, 1990 The *tra-1* gene determines sexual phenotype cell-autonomously in C. elegans. Cell **63:** 1193–1204.

HUNTER, C. P., and W. B. WOOD, 1992 Evidence from mosaic analysis of the masculinizing gene *her-1* for cell interactions in *C. elegans* sex determination. Nature **355:** 551–555.

JOHNSTONE, I. L., 1994 The cuticle of the nematode *Caenorhabditis elegans*: a complex collagen structure. BioEssays **16:** 171–178.

KENYON, C., 1986 A gene involved in the development of the posterior body region of C. elegans. Cell **46:** 477–481.

KIMBLE, J., and D. HIRSH, 1979 The post-embryonic cell lineages of the hermaphrodite and male gonads of *Caenorhabditis elegans*. Dev. Biol. **70:** 396–417.

KRAMER, J. M., 1994 Structures and functions of collagens in *Caenorhabditis elegans*. FASEB J. **8:** 329–336.

KRAUSE, M., S. W. HARRISON, S.-Q. XU, L. CHEN and A. FIRE, 1994 Elements regulating cell- and stage-specific expression of the *C. elegans* MyoD family homolog *hlh-1*. Dev. Biol. **166:** 133–148.

LACKNER., M. R., K. KORNFELD, L. M. MILLER, H. R. HORVITZ and S. K. KIM, 1994 A MAP kinase homolog, *mpk-1*, is involved in *ras*-mediated induction of vulval cell fates in *Caenorhabditis elegans*. Genes Dev. **8:** 160–173.

LEUNG-HAGESTEIJN, C., A. M. SPENCE, B. D. STERN, Y. ZHOU, M.-W. SU *et al.*, 1992 UNC-5, a transmembrane protein with immunoglobulin and thrombospondin type 1 domains, guides cell and pioneer axon migrations in C. elegans. Cell **71:** 289–299.

MCKIM, K. S., and A. M. ROSE, 1990 Chromosome *I* duplications in *Caenorhabditis elegans*. Genetics **124:** 115–132.

MELLO, C. C., J. M. KRAMER, D. STINCHCOMB and V. AMBROS, 1991 Efficient gene transfer in *C. elegans*: extrachromosomal maintenance and integration of transforming sequences. EMBO J. **10:** 3959–3970.

PALMER, R. E., E. HOGAN and D. KOSHLAND, 1990 Mitotic transmission of artificial chromosomes in *cdc* mutants of the yeast, *Saccharomyces cerevisiae*. Genetics **125:** 763–774.

PERKINS, L. A., E. M. HEDGECOCK, J. N. THOMSON and J. G. CULOTTI, 1986 Mutant sensory cilia in the nematode *Caenorhabditis elegans*. Dev. Biol. **117:** 456–487.

ROSENBLUTH, R. E., C. CUDDEFORD and D. L. BAILLIE, 1985 Mutagenesis in *Caenorhabditis elegans*. II. A spectrum of mutational events induced with 1500 R of g-irradiation. Genetics **109:** 493–511.

SEYDOUX, G., and I. GREENWALD, 1989 Cell autonomy of *lin-12* function in a cell fate decision in C. elegans. Cell **57:** 1237–1245.

SEYDOUX, G., T. SCHEDL and I. GREENWALD, 1990 Cell-cell interactions prevent a potential inductive interaction between soma and germline in C. elegans. Cell **61:** 939–951.

SIMSKE, J. S., and S. K. KIM, 1995 Sequential signaling during *Caenorhabditis elegans* vulval induction. Nature **375:** 142–146.

STERNBERG, P. W., 1993 Intercellular signaling and signal transduction in *C. elegans*. Annu. Rev. Genet. **27:** 497–521.

STINCHCOMB, D. T., J. E. SHAW, S. H. CARR and D. HIRSH, 1985 Extrachromosomal DNA transformation of *Caenorhabditis elegans*. Mol. Cell. Biol. **5:** 3484–3496.

SULSTON, J., and J. HODGKIN, 1988 Methods, pp. 587–606 in *The Nematode Caenorhabditis elegans*, edited by W. B. WOOD. Cold Spring Harbor Laboratory, Cold Spring Harbor, NY.

SULSTON, J. E., and H. R. HORVITZ, 1977 Postembryonic cell lineages of the nematode *Caenorhabditis elegans*. Dev. Biol. **56:** 110–156.

SULSTON, J., and J. WHITE, 1988 Parts list, pp. 415–431 in *The Nematode Caenorhabditis elegans*, edited by W. B. WOOD. Cold Spring Harbor Laboratory, Cold Spring Harbor, NY.

SULSTON, J. E, E. SCHIERENBERG, J. G. WHITE and J. N. THOMSON, 1983 The embryonic cell lineage of the nematode *Caenorhabditis elegans*. Dev. Biol. **100:** 64–119.

SULSTON, J., H. R. HORVITZ and J. KIMBLE, 1988 Cell lineage, pp. 457–489 in *The Nematode Caenorhabditis elegans*, edited by W. B. WOOD. Cold Spring Harbor Laboratory, Cold Spring Harbor, NY.

THOMAS, J. H., M. J. STERN and H. R. HORVITZ, 1990 Cell interactions coordinate the development of the C. elegans egg laying system. Cell **62:** 1041–1052.

VILLENEUVE, A. M., and B. J. MEYER, 1990 The role of *sdc-1* in the sex determination and dosage compensation decisions in *Caenorhabditis elegans*. Genetics **124:** 91–114.

WARING, D. A., and C. KENYON, 1991 Regulation of cellular responsiveness to inductive signals in the developing *C. elegans* nervous system. Nature **350:** 712–715.

WHITE, J. G., E. SOUTHGATE, J. N. THOMSON and S. BRENNER, 1986 The structure of the nervous system of *Caenorhabditis elegans*. Philos. Trans. R. Soc. Lond. B Biol. Sci. **314:** 1–340.

YUAN, J. Y., and H. R. HORVITZ, 1990 The *Caenorhabditis elegans* genes *ced-3* and *ced-4* act cell autonomously to cause programmed cell death. Dev. Biol. **138:** 33–41.

Communicating editor: I. GREENWALD